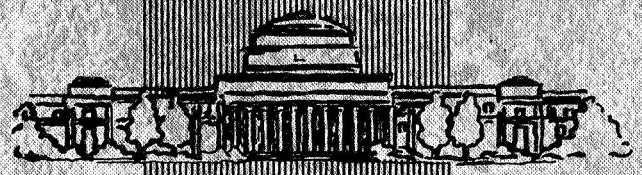

# MASSACHUSETTS INSTITUTE OF TECHNOLOGY

TE-27

## SPIN-ORBIT RESONANCE OF MERCURY

by

Charles Claude Counselman III

February 1969

Degree of Doctor of Philosophy

EXPERIMENTAL ASTRONOMY LABORATORY
MASSACHUSETTS INSTITUTE OF TECHNOLOGY
CAMBRIDGE 39, MASSACHUSETTS

TE-27

# SPIN-ORBIT RESONANCE OF MERCURY

by

CHARLES CLAUDE COUNSELMAN, III

B.S., M.I.T., 1964

M.S., M.I.T., 1965

SUBMITTED IN PARTIAL FULFILLMENT
OF THE REQUIREMENTS FOR THE
DEGREE OF DOCTOR OF PHILOSOPHY

at the

MASSACHUSETTS INSTITUTE OF TECHNOLOGY

February, 1969

Signature of Author Charles Claude Counselman III
Department of Aeronautics and Astronautics,
December 30, 1968

Certified by Irwin Shapiro
Thesis Supervisor

Certified by Alar Toomre
Thesis Supervisor

Certified by Walter Wrigley
Thesis Supervisor

Accepted by Walter Wrigley
Chairman, Departmental Committee on Graduate Students

SPIN-ORBIT RESONANCE OF MERCURY

by

Charles Claude Counselman III

Submitted to the Department of Aeronautics and Astronautics in February, 1969 in partial fulfillment of the requirement for the degree of Doctor of Philosophy.

ABSTRACT

The present oscillations in orbital eccentricity, if considered typical for geologic time periods, imply that the probability of Mercury's having evolved to the 3:2 spin-orbit resonance state is only about 0.02. This probability is too low to be believable and indicates that the two-dimensional mathematical model hitherto used to describe the evolution into resonance may be seriously in error. Mercury's average orbital eccentricity (now 0.18) may have been significantly higher ($>0.25$) in the distant past, or, perhaps, Mercury has a liquid core dissipatively coupled to its mantle. The first possibility, if realized, would yield a high capture probability but requires extensive calculations and has not yet been explored. Investigation of the second showed that the probability of penetration of the higher resonances, with subsequent capture into the 3:2 state, is only appreciable ($\gtrsim 0.5$) for a very narrow range of core-mantle coupling constants. For a core whose moment of inertia is one-tenth that of the mantle, the capture probability is a maximum for coupling with a characteristic relaxation time of about 40,000 years. A three-dimensional model might lead to significantly different capture probabilities but has not yet been analyzed.

Included in the thesis is a critical discussion of tidal models appropriate for planetary spin-orbit resonance problems.

Thesis Supervisors:

Irwin I. Shapiro, Ph.D.
Title: Professor of Geophysics and Physics

Alar Toomre, Ph.D.
Title: Associate Professor of Applied Mathematics

Walter Wrigley, Sc.D.
Title: Professor of Instrumentation and Astronautics

ACKNOWLEDGEMENTS

I wish to thank the members of my thesis committee, Professors Shapiro, Toomre, and Wrigley, for their support and encouragement. I am grateful to Professor Walter Wrigley, chairman of the interdepartmental Instrumentation doctoral program and my graduate program advisor, who encouraged a thesis in astronomy, and to Alar Toomre for his reviews of my mathematical arguments. My greatest debt I owe to Irwin Shapiro, for his constant advice and criticism at every stage of the research, and for his personal inspiration and encouragement.

To my colleagues at the Experimental Astronomy Laboratory, Renwick E. Curry, Neal A. Carlson, and Stephen J. Madden, I am grateful for countless helpful consultations on mathematics and computer programming. Dr. Robert G. Stern, my supervisor at E.A.L., has provided a stimulating research environment, for which I am grateful. I thank Toni Forni for her help in running computer programs at M.I.T. Lincoln Laboratory.

Most of all I thank my wife, Eleanor, for attending to many of my responsibilities while I completed this research.

Computation was done at the M.I.T. Computation Center under problem number M4323. This research was supported in part by grant NsG 254-62 from the National Aeronautics and Space Administration.

The excellent typing of this paper has been done by Ann Archer.

## BIOGRAPHICAL NOTE

Charles Claude Counselman III was born in Baltimore, Maryland on 27 April, 1943. He graduated from Loyola High School, Towson, Maryland in 1960, and has attended the Massachusetts Institute of Technology since that year. He received the B.S. in Electrical Engineering in 1964 and the M.S. in Electrical Engineering in 1965.

His graduate study has been supported by a National Science Foundation Fellowship (1964-1965), Sperry Gyroscope Fellowship (1965-1966), and by a research assistantship at the M.I.T. Experimental Astronomy Laboratory (1966-68). During summers he has been employed as staff member in the M.I.T. Instrumentation Laboratory (1965), Experimental Astronomy Laboratory (1966), and Lincoln Laboratory (1968). He has worked in the areas of electronics, inertial guidance, celestial mechanics, lunar and planetary radar astronomy.

He was married to Eleanor Frey, of Baltimore, Maryland in June, 1966. His wife is a doctoral candidate at Boston University.

SPIN-ORBIT RESONANCE OF MERCURY

TABLE OF CONTENTS

# SPIN-ORBIT RESONANCE OF MERCURY

## I. Introduction

Radar observations have revealed that Mercury's axial rotation is direct with a sidereal period of 59 ± 3 days (Pettengill and Dyce, 1965; Dyce, Pettengill, and Shapiro, 1967), rather than the previously accepted value of 88 days (see, for example Dollfus, 1953). Peale and Gold (1965) first proposed an explanation for this 59-day period solely in terms of tidal torques; with an orbital eccentricity of 0.2 Mercury's orbital angular velocity at perihelion slightly exceeds its spin rate so that the tidal torque on the planet would be reversed in direction during just that portion of the orbit when tidal interaction is strongest. Although the planet does spend more time near aphelion than perihelion, the average tidal torque could vanish for a rotation period of about 59 days, resulting in a stable spin state. Colombo (1965) pointed out, however, that the observed spin period was almost exactly 2/3 of an orbital period, or 58.65 days. He suggested that a nearly uniform rotation at just 3/2 the mean orbital angular velocity might actually be stabilized if Mercury had a slight permanent equatorial asymmetry. Approximate analyses by Colombo and Shapiro (1965) and soon after by others (Liu and O'Keefe, 1965; Goldreich and Peale, 1966a; Laslett and Sessler, 1966; Jefferys, 1966) confirmed that such a spin-orbit resonance could, under certain conditions, be stable.

An average spin period exactly 2/3 of an orbital period is also consistent with many optical observations of Mercury (McGovern, Gross, and Rasool, 1965; Colombo and Shapiro, 1965; Camichel and Dollfus, 1967; Chapman, 1967). Due to their quality and their spacing in time, these optical observations are somewhat ambiguous; i.e. much of the data appears to allow multiple solutions for the spin period (hence partially explaining the earlier 88-day result). But the purely statistical uncertainty of a given single solution may be quite small -- perhaps 0.01 days (Camichel and Dollfus 1967). Radar measurements of the spin rate based on delay-Doppler mapping (Dyce, Pettengill and Shapiro, 1967) are less precise, but have no such

ambiguity. The radar and optical data taken together suggest that a spin-orbit resonance condition in fact exists, with Mercury completing three axial rotations with respect to the "fixed"stars, and one rotation with respect to the sun, in two orbital periods.

In this paper we compute the probability that Mercury's spin state would evolve into this resonance, for a variety of a priori assumptions regarding the long-term variations of Mercury's orbit, the behavior of the tidal torque, the size of the permanent equatorial asymmetry of Mercury's inertia ellipsoid, and the possible existence and nature of a fluid core within Mercury. The resulting computed probabilities allow us to identify the most likely physical properties and parameter values from among the various a priori possibilities considered. Many can be excluded because they lead to a vanishing probabilities of occurrence of the 3:2 spin-orbit resonance.

One might ask how probability enters into this problem, to which deterministic classical mechanics presumably applies. After all, in classical mechanics the equations of motion of a dynamical system and the specified initial conditions determine the state at a later time with no randomness. For the spin state of Mercury, however, we find that incredibly small variations, either in the "initial" state of motion or in the values of parameters in the equations of motion, affect decisively the final (stable) state of the system, which usually corresponds to Mercury either being in a spin-orbit resonance, or rotating at the rate for which the tidal torque itself averages to zero. It is our ignorance of these initial conditions and parameter values for the planet Mercury which makes only a statistical treatment reasonable.

Goldreich and Peale (1966b) were the first to publish calculations of the probability for Mercury to be captured into the 3:2 spin-orbit resonance state; they considered several tidal-friction models and a range of fixed values of orbital eccentricity. The effect of a fluid core within Mercury was not considered, although in a later paper, Goldreich and Peale (1967) computed the effect of core-mantle coupling in the planet Venus on the probability of capture of Venus' spin into a resonance with

the relative orbital motion of the Earth and Venus. Goldreich and Peale (1966b) also discussed the applicability of their Mercury calculations, in which the orbital eccentricity $e$ was fixed, to the real case in which planetary perturbations cause secular variations of the orbital elements. [According to calculations by Brouwer and van Woerkom (1950), Mercury's eccentricity can vary between approximately 0.12 and 0.24 in a few hundred thousand years, due principally to perturbations by Venus and Jupiter.] Clearly if the rate of change of eccentricity is sufficiently slow, the capture probability may be calculated for fixed values of the eccentricity with the effective capture probability being an appropriate (weighted) average over the separate values for each eccentricity that can occur. Less obvious is the proper simplification for the opposite extreme case, in which de/dt is so large that the eccentricity goes through many oscillations while the spin state remains in the neighborhood of a resonance. Having performed several thousand Monte Carlo trials on a computer, Goldreich and Peale (1966b) concluded for this case "with some confidence that the over-all capture probability in an orbit of varying eccentricity is intermediate between the largest and smallest values of the capture probability (calculated for fixed orbits) over the range of eccentricity." For the eccentricity variation determined by Brouwer and van Woerkom (1950) for Mercury, these largest and smallest values of the capture probability, for the model used by Goldreich and Peale, are nearly one and zero, respectively; hence their conclusion, although unassailable, is not particularly useful. Moreover as they also realized, the actual value of de/dt for Mercury lies between these limiting cases. A theory of resonance capture is clearly needed which includes such orbital element variations.

In this paper we consider the rotation of Mercury near a spin-orbit resonance, developing a theory which encompasses possible variations in orbital eccentricity as well as core-mantle coupling. Formulae are derived for computing the probability of capture into a resonance and are applied for various tidal models and for a range of values of the tidal dissipation factor "Q", the permanent equatorial asymmetry (B-A)/C of Mercury's inertia ellipsoid, the core moment of inertia, and the effective core-mantle viscosity.

## II. MATHEMATICAL MODEL

We will assume that Mercury's axis of rotation has always remained normal to its orbital plane and so will neglect the effects of obliquity in our analysis. The possible evolution of the direction of the planet's spin axis and the effects of varying orbital inclination will be considered in a separate publication.

### A. Torques

Mercury's rotational state is, of course, influenced by the totality of torques acting on it. We consider only the two which seem most important (Colombo and Shapiro, 1965): The torques exerted by the sun on a permanent equatorial asymmetry of Mercury's moment of inertia ellipsoid and on the tidal bulge raised by the sun. We discuss each in turn. Defining Mercury's three principal moments of inertia as A, B, and C, and assuming that the planet's spin axis coincides with the body axis of maximum moment of inertia C(C>B>A), we find that the torque exerted by the sun on this permanent asymmetry is given to sufficient precision by MacCullagh's formula (see, e.g., Danby, 1962)

$$T_{pa} = -\frac{3}{2}\frac{GM_{\odot}}{r^3}(B - A)\sin 2(\theta - v)\hat{k} \quad , \tag{1}$$

where $\hat{k}$ is a unit vector parallel to the spin axis, (B-A) is the difference between the two equatorial moments, G is the gravitational constant, $M_{\odot}$ is the mass of the Sun, and $r$ is the Sun-Mercury distance. Figure 1 shows that $(\theta - v)$ is, by definition, the difference between the orbital true anomaly $v$ and the angle $\theta$ between the axis of minimum moment of inertia of the planet and the orbit major axis.

The other external torque likely to be significant is the tidal drag torque (Darwin, 1908). The tidal torque is analogous to the asymmetry torque just discussed, the main difference being that the asymmetry in this case is not a permanent one but is due to the deformation of the

non-rigid planet by the differential solar gravitational field. In a mechanically lossless planet the tidally induced long axis ("high tide") always points directly towards the sun, so that the torque due to the tidally-induced asymmetry vanishes (cf. Eq. 1). If there is internal dissipation, however, the motion of the tidal bulge lags behind the motion of the planet-sun direction, the dissipated energy being supplied by the rotation of the planet.

The detailed mechanisms of tidal dissipation are uncertain, even for the Earth, but it is possible to estimate the magnitude of the gross effect (see, for example, MacDonald, 1964; Goldreich and Soter, 1966). For our purposes the tidal torque is adequately described by its magnitude (its sense is assumed to be opposed to the planet's rotation as seen from the sun) and the manner in which this magnitude depends on, for example, the rate of rotation. In Appendix A, we show that the tidal torque can be written as

$$\vec{T}_t = -\frac{45}{8}(\mu_T+1)^{-1}\left(\frac{n^4RC}{g}\right)\left(\frac{a}{r}\right)^6 \sin 2\delta\ \hat{k}\ , \qquad (2)$$

where $n$ is Mercury's orbital mean motion, $a$ its orbital semimajor axis, R its radius, $g$ the acceleration of gravity on its surface, $\mu_T$ its tidal effective rigidity, and $\delta$ the tidal lag angle. The relation of this angle to Mercury's effective "Q"

$$\sin 2\delta = \left(\frac{\mu_T}{\mu_T + 1}\right) Q^{-1} \quad , \qquad (3)$$

is also derived in Appendix A.

How does the tidal lag angle (or the Q) of Mercury vary with the spin rate, or with the amplitude of the tidal strain? Unfortunately the answer is unknown and we will therefore examine three models for the lag angle: (1) $\delta$ constant; (2) $\delta$ proportional to the rate; and (3) $\delta$ proportional to the amplitude of the tidal strain. The first was

considered by Colombo and Shapiro (1965) and all three by Goldreich and Peale (1966). Clearly other models could be constructed, but these three should prove representative.

If the tide always lags the sun by a constant angle $\delta$, independent of the amplitude or rate of the tidal strain (model 1), Eq. (2) can be written as

$$T_t/n^2C = -\alpha(a/r)^6 \operatorname{sgn}\left[\frac{d\theta}{dM} - \frac{dv}{dM}\right] = -\alpha\left(\frac{1+e\cos v}{1-e^2}\right)^6 \operatorname{sgn}\left[\frac{d\theta}{dM} - \frac{dv}{dM}\right] \tag{4}$$

in which $M = nt$ is the orbital mean anomaly and $\alpha$ is a small positive dimensionless constant:

$$\alpha = \frac{45}{8}\,\frac{\mu_T}{(\mu_T + 1)^2}\left(\frac{n^2R}{g}\right) Q^{-1} \approx 2 \times 10^{-7}\, Q^{-1} \tag{5}$$

where in the last relation we assume $\mu_T \approx 20$ (see Appendix A). The division by $n^2C$ makes both sides of Eq. (4) dimensionless; this form will be useful below. We may place an approximate lower bound on $\alpha$ (upper bound on Q) by the following argument (Colombo and Shapiro, 1965). Assuming that Mercury's Q has been constant since the planet was formed (about $4.5 \times 10^9$ years ago), that Mercury's spin period was then about 20 hours, and that solar tidal friction was wholly responsible for the slowing of the spin rate, we find that

$$\frac{d^2\theta}{dt^2} \approx -\alpha\, n^2 \tag{6}$$

requires

$$\alpha \gtrsim 10^{-9} \tag{7}$$

or

$$Q \lesssim 200 \tag{8}$$

This bound on Q is about the same as that implied by laboratory studies on rocks and by seismic studies of the Earth's mantle. (See Appendix A.)

For model 2, we assume that the tidal dissipation is viscous or, equivalently, that $Q^{-1} \propto \delta \propto \left|\frac{d\theta}{dM} - \frac{dv}{dM}\right|$. The corresponding mechanical behavior is that of a linear, damped oscillator. Thus,

$$T_t/n^2C = -\alpha \left(\frac{1+e \cos v}{1 - e^2}\right)^6 \left(\frac{d\theta}{dM} - \frac{dv}{dM}\right) , \tag{9}$$

where $\alpha$ is again a small positive constant.

Because the tide-raising potential varies as $r^{-3}$, Mercury's orbital eccentricity of 0.2 causes the tidal amplitude at perihelion to be about 3.4 times greater than at aphelion. Therefore, an amplitude dependence of dissipation mechanisms could be significant for Mercury. If the planet's Q is taken inversely proportional to the strain amplitude (model 3), we obtain

$$T_t/n^2C = -\alpha \left(\frac{1+e \cos v}{1 - e^2}\right)^9 \operatorname{sgn}\left(\frac{d\theta}{dM} - \frac{dv}{dM}\right) \tag{10}$$

in which $\alpha$ represents the small positive constant.

B. Equation of Motion

In our discussion of the spin equation of motion we take the tidal torque from Eq. (4). The results of this section will, however, apply as well to the other tidal torque formulae, (9) and (10).

With Eq. (1) representing the torque attributable to the permanent asymmetry, the spin equation of motion may be written after division by $n^2C$ throughout, as

$$\frac{d^2\theta}{dM^2} = -\beta \left(\frac{1+e \cos v}{1 - e^2}\right)^3 \sin 2(\theta - v) - \alpha \left(\frac{1+e \cos v}{1 - e^2}\right)^6 \operatorname{sgn}\left(\frac{d\theta}{dM} - \frac{dv}{dM}\right) , \tag{11}$$

where here and in what follows we use the dimensionless orbital mean anomaly, M, rather than time as the independent variable, and introduce

the asymmetry parameter $\beta$:

$$\beta \equiv \frac{3}{2} \frac{(B-A)}{C} \quad . \tag{12}$$

Eq. (11) is not solvable in closed form. An approximate solution can be obtained easily because $\alpha, \beta << 1$; thus, in one orbital period (M increased by $2\pi$) the change in the dimensionless spin rate $d\theta/dM$ must be small compared to unity. We may therefore integrate the right side of (11) over an orbital period holding $d\theta/dM$ constant in the integration, to eliminate the time dependence introduced by $v$. For this purpose the notation of Bellomo, Colombo and Shapiro (1966) is useful. The functions appearing on the right side of Eq. (11) are denoted by $P(e, \theta, M)$ and $T(e, \omega, M)$ where

$$P(e,\theta,M) \equiv - \left(\frac{1+e \cos v}{1-e^2}\right)^3 \sin 2(\theta - v) \quad , \tag{13}$$

$$T(e,\omega,M) \equiv - \left(\frac{1+e \cos v}{1 - e^2}\right)^6 \operatorname{sgn} \left(\omega - \frac{dv}{dM}\right) \tag{14}$$

and

$$\omega \equiv \frac{d\theta}{dM} \quad . \tag{15}$$

Assuming $\omega$ to be constant in $T(e,\omega,M)$, we may integrate to obtain the average value $T_0(e,\omega)$:

$$T_0(e,\omega) \equiv \frac{1}{2\pi} \int_0^{2\pi} T(e,\omega,M)dM \tag{16}$$

where the zero subscript indicates the zero-th coefficient in a Fourier series expansion in M of the periodic function T. In spite of the seeming complexity of the function T, the integral in (16) may be carried out analytically to obtain closed-form expressions for the average dimensionless tidal torque $T_0$ for each of the three models previously discussed.

The resulting expressions for $T_0(e,\omega)$ are given in Appendix B.

Before integrating $P(e,\theta,M)$, we express $\theta(M)$ in terms of an initial value $\theta_0 \equiv \theta(0)$ and an (assumed constant) angular rate $\omega$. Because of our interest in resonances, we at first consider only half-integer values of $\omega$, or

$$\omega = \frac{k}{2} \quad , \quad k = \ldots, -2, -1, 0, 1, 2, 3, \ldots \tag{17}$$

We observe that $P(e,\theta_0 + kM/2,M)$ is a periodic function of M having period $2\pi$. The result of an integration over an orbital period may be expressed simply as

$$-P_k(e) \sin 2\theta_0 = \frac{1}{2\pi} \int_0^{2\pi} P(e,\theta_0 + kM/2,M)dM \ , \tag{18}$$

where $P_k$ is a function of only the orbital eccentricity e. The functions $P_k(e)$ have been derived by Bellomo et al. (1966) for k = -3, -2,... ..,7. Goldreich and Peale (1966b) have pointed out that coefficients of series expansions in e through $e^7$ for such functions as $P_k(e)$ are given in Cayley's (1859) tables. An expression valid for arbitrary k is presented by Counselman and Shapiro (1969).

The angle $\theta_0$ appearing in Eq. (18) is the instantaneous value of $\theta$ at perihelion passage (M = 0). If indeed $\omega$ = constant = k/2, then $\theta = \theta_0 (\text{mod } \pi)$ at successive perihelia (M = $2n\pi$, n = 1,2,3...). The orientation of the planet's principal axes of inertia with respect to the orbit major axis is thus precisely the same at every successive perihelion passage when $\omega$ is a half-integer. For $\omega$ at or near a half-integer value, it is useful to imagine the planet's rotation as being observed stroboscopically, i.e. only at perihelion passage, and to define the instantaneous orientation observed there as $\theta'$. A so-called "resonance" rotation state is characterized by a fixed value of $\theta'$. If the actual rotation rate $\omega$ is nearly equal to a half-integer then $\theta'$

will appear (stroboscopically) to be slowly varying. We may then define derivatives of $\theta'$ by

$$\left.\begin{aligned} \frac{d\theta'}{dM} &= \left\langle \frac{d\theta}{dM} - \frac{k}{2} \right\rangle \\ \frac{d^2\theta'}{dM^2} &= \left\langle \frac{d^2\theta}{dM^2} \right\rangle \end{aligned}\right\} , \tag{19}$$

where the angle brackets signify averages taken over an orbital period. The long-term behavior of $\theta'$ is given approximately by the solution of the differential equation obtained by substituting the averaged expressions (16), (18), and (19) for the corresponding (unaveraged) quantities in Eq. (11). We obtain

$$\frac{d^2\theta'}{dM^2} = -\beta P_k(e) \sin 2\theta' + \alpha T_0\left(e, \frac{k}{2} + \frac{d\theta'}{dM}\right) \tag{20}$$

Because $d\theta'/dM$ is small, $T_0$ may be expanded near $\omega = k/2$. Defining

$$T_0'(e,k/2) \equiv \left[\frac{\partial}{\partial\omega} T_0(e,\omega)\right]_{\omega=k/2} , \tag{21}$$

and dropping the prime on $\theta$, we may write

$$\frac{d^2\theta}{dM^2} + \beta P_k(e) \sin 2\theta = \alpha T_0(e,k/2) + \alpha T_0'(e,k/2) \frac{d\theta}{dM} . \tag{22}$$

For a given resonance number k and eccentricity e, the coefficients $P_k$, $T_0$, and $T_0'$ are constant. The near-resonance motion is seen to obey a simple "pendulum" equation, to which a constant term and a term proportional to rate have been added on the right side.

Eq. (22) is equivalent to the averaged equation derived earlier by Goldreich and Peale (1966b). Our derivation makes more evident the assumptions involved and allows one to compare the averaged equations with the difference equations derived by Bellomo et al. (1966).

Before discussing these assumptions, we describe the properties of the solution to Eq. (22). Evidently the nature of the solution depends on the relative magnitudes of the constants $\alpha$, $\beta$, $P_k$, $T_0$, and $T_0'$. The constants $\alpha$ and $\beta$ are small: $\alpha$ depends on the planet's tidal Q, which is unknown, but $\alpha$ may be expected to be in the range from $10^{-8}$ to $10^{-9}$ (Q between 20 and 200); $\beta$, also unknown, would be $3 \times 10^{-4}$, if Mercury's equatorial asymmetry were as large as the moon's. For the Earth, $\beta \approx 10^{-5}$. Thus we can expect $\alpha$ and $\beta$ to satisfy $\alpha << \beta << 1$, with $\alpha$ probably on the order of $\beta^2$. The parameter $P_k$ depends only on the orbital eccentricity e, for a specified resonance number k. For the 59-day resonance (k=3), $P_k = 0.64$ when $e = 0.2$; usually $P_k$ is on the order of unity. The parameters $T_0$ and $T_0'$ depend on the choice of tidal model as well as on the orbital eccentricity and resonance number. We will be concerned primarily with physical conditions for which $T_0 \approx -1$ and $-1 \lesssim T_0' \leq 0$. The parameters $\alpha$ and $\beta$ are thus much less than unity, whereas the magnitudes of $P_k$, $T_0$, and $T_0'$ are usually of the order of unity.

By analogy with the familiar behavior of a pendulum, we now review briefly the qualitative behavior of the solution to Eq. (22), here rewritten in simplified form with a dot notation signifying differentiation with respect to M:

$$\ddot{\theta} + \beta P_k \sin 2\theta = \alpha(T_0 + T_0'\dot{\theta}) \tag{23}$$

This review will be helpful in understanding the discussions in the following sections.

Clearly, two equilibrium points exist in the interval $-\pi/2 < \theta \leq \pi/2$. The equation is satisfied if $\dot{\theta} = 0$ and

$$\theta = \theta_{eq} = \frac{1}{2} \sin^{-1}(\alpha T_0/\beta P_k) \quad . \tag{24}$$

Since $|\alpha T_0| << \beta P_k$, we have

$$\theta_{eq} \approx \alpha T_0/2\beta P_k \quad , \tag{25}$$

or

$$\theta_{eq} \approx -\pi/2 - \alpha T_0/2\beta P_k \quad . \tag{26}$$

Straightforward linear stability analysis (Bellomo et al., 1967) shows that if $P_k(e) > 0$, the fixed point (26) is always unstable, and that if $T_0' < 0$, the other fixed point (25) is asymptotically stable. Small oscillations about (25) have a circular frequency approximately $(2\beta P_k)^{1/2}$ and decay as exp $(\alpha T_0' M/2)$ with M approaching infinity.

If $\alpha = 0$ (or if $\alpha \neq 0$, but $T_0' = 0$), an energy integral exists (Goldreich and Peale, 1966b). It is easily verified by substitution that

$$E(\theta,\dot{\theta}) = \frac{1}{2} (\dot{\theta})^2 - \beta P_k \cos^2\theta \tag{27}$$

is an integral of (23) if $\alpha = 0$; if $\alpha \neq 0$ but $T_0' = 0$, then $(E - \alpha T_0 \theta)$ is an integral. The first and second terms in (27) may be identified as a kinetic and potential energies, respectively. Eq. (23) thus describes the one-dimensional conservative motion of a classical particle in a periodic potential $-\beta P_k \cos^2\theta$ if $\alpha = 0$; if $\alpha \neq 0$, but $T_0' = 0$, a slight uniform slope is superimposed on the periodic potential pattern. The equilibrium solutions (26) and (25) clearly correspond, respectively, to particles balanced on the top of a potential "hump" and resting stably in the bottom of a potential "well". In the particle-potential-well analogy, a particle confined to one of the periodically spaced "wells" represents Mercury trapped in a spin-orbit resonance. The planet rotating faster than the half-integer resonance rate but being decelerated by the tidal torque $(T_0 + T_0'\dot{\theta} < 0)$ is represented by a particle moving through a force field composed of the gradient of a periodic potential and a slight, velocity dependent drag term. Eventually the drag term absorbs all of the particle's kinetic energy and it stops at a point corresponding to the "uphill" side of a potential well and begins to fall backward. The subsequent motion will depend critically on the coefficient $T_0'$. If $T_0' = 0$ the dynamic system is exactly reversible in time: the particle's subsequent motion is just the reverse of that which pre-

ceded the moment of zero velocity. The energy subtracted by the $T_0$ term is replaced in full during the reversed motion. The analogous planet slows to the resonance spin rate and passes on, continuing to decelerate. If, on the other hand, $T_0' < 0$, this term causes dissipation both as the particle moves forward before stopping, and again as it moves backwards through the same periodic potential. Depending on how much energy is lost in the "final" well and on just how much kinetic energy the particle had when entering the last well, the "reversed" particle may or may not be able to escape from this final well. If it escapes, the particle will keep on going backwards; if not, it will be trapped, moving back and forth with ever-decreasing oscillations, tending asymptotically toward the stable equilibrium position ($\theta_{eq} = \alpha T_0/2\beta P_k$) corresponding to the bottom of the well. The planet corresponding to the trapped particle reaches the resonance spin rate and passes it only temporarily, with the instantaneous spin rate performing ever-decreasing oscillations about the resonance value. At final equilibrium the planet rotates by a half-integral number of times per orbit, and the planet's equatorial principal axis of minimum inertia makes an angle with the orbit major axis at perihelion passage of just $\theta_{eq} = \alpha T_0/2\beta P_k$ for $P_k(e) > 0$.

Assuming that the initial kinetic energy of the particle is a uniformly distributed random variable, we can easily compute the "capture" probability for the particle, i.e. the probability that the particle becomes trapped in the well where it first stops, rather than rolling backwards out of this well. The probability of capture is obtained by considering the possible range of kinetic energy of the particle as it enters the final well, and by comparing this range with the energy dissipated in the final well due to $T_0'$ being negative (Goldreich and Peale, 1966b).

If we denote the particle's position by $\theta$, in analogy with the variable describing the axis orientation at perihelion in the planet case, then the particle's motion through the final (nth) well is bounded by the unstable fixed points (near the potential maxima) at

$\theta_n = (n - \frac{1}{2})\pi - \alpha T_0/2\beta P_k$ and $\theta_{n+1} = (n + \frac{1}{2})\pi - \alpha T_0/2\beta P_k$. For this to be the final well, the kinetic energy of the particle as it passes $\theta_n$ must be less than $\varepsilon$, where

$$\varepsilon \equiv \pi\alpha|T_0|, \tag{28}$$

plus whatever energy the $T_0'$ term causes to be dissipated in the motion from $\theta_n$ to $\theta_{n+1}$. This dissipation is velocity-dependent, but the velocity of the particle in the final well is given approximately by Eq. (27), with the constant E appropriate for the conditions existing at the particle's entry into the final well. Since the kinetic energy will vanish in this final well due to dissipation caused by forces proportional to $\alpha$, and since $\alpha << \beta$, we must have $E << \beta P_k$ in the final well. Therefore, we set E = 0 in (27) and solve for $\dot{\theta}$ in terms of $\theta$:

$$\dot{\theta} \approx (2\beta P_k)^{1/2}\cos\theta \tag{29}$$

The energy dissipated as $\theta$ increases from $\theta_n$ to $\theta_{n+1}$ is approximately $\delta$, where

$$\delta \equiv \int_{\theta_n}^{\theta_{n+1}} \alpha|T_0'|\dot{\theta}d\theta \tag{30}$$

(We are assuming, of course, that $T_0' < 0$.) Substituting (29) into (30) and integrating yields

$$\delta \approx 2\alpha|T_0'|(2\beta P_k)^{1/2} . \tag{31}$$

Thus at $\theta = \theta_n$ the kinetic energy $K_n$ must lie in the range

$$0 < K_n < -\pi\alpha T_0 - 2\alpha T_0'(2\beta P_k)^{1/2} = \varepsilon + \delta \quad , \tag{32}$$

in order for the kinetic energy to vanish within the nth well. The particle will be trapped there unless $K_n$ actually exceeds $2\delta$ because the $T_0'$ dissipative effect acts independently of the sign of $\dot{\theta}$ and hence is cumulative over the forwards and backwards motion within the nth well.

If all values of $K_n$ in the range (32) are equally likely, then the capture probability P {capture} is simply

$$P\ \{\text{capture}\} = 2\delta/(\varepsilon + \delta) \quad , \tag{33}$$

as first given by Goldreich and Peale (1966b). If (33) yields a value greater than 1, then of course P {capture} = 1. Hence capture becomes certain when $\delta \geq \varepsilon$. This condition has an appealing and useful interpretation in terms of what may be called the "width" of the resonance,

$$\omega_\beta = (2\beta P_k)^{1/2} \quad . \tag{34}$$

This width $\omega_\beta$ is equal to the circular frequency of small oscillations about the stable point (25). It is also equal to the amplitude of the variation in the (average) spin rate $\dot{\theta}$ when the planet is first trapped in the final well, as seen in Eq. (29). The condition $\delta \geq \varepsilon$ may be written in terms of $\omega_\beta$ as

$$\left| \frac{2T_0'\omega_\beta}{\pi T_0} \right| \geq 1 \tag{35}$$

We see that capture is certain if twice the variation in tidal torque across one resonance width exceeds $\pi$ times the (average) value of the tidal torque at the center of the resonance. Because $\omega_\beta$ is so small ($\omega_\beta \approx 10^{-2}$ when $\beta = 10^{-4}$), the inequality (35) requires $|T_0'| >> |T_0|$. Because $|T_0'|$ is of the order of unity for plausible tidal models and reasonable values of orbital eccentricity, large capture probability evidently requires that $|T_0| << 1$; in other words, for capture to be likely, the resonance spin rate must be very nearly equal to that spin rate for which the average tidal torque vanishes. Since the latter rate is just the same equilibrium rate that would result in the absence of an equatorial asymmetry ($\beta = 0$), it would appear that resonance capture does not alter the equilibrium rate substantially. Resonance capture will be likely only at spin rates within a narrow "resonance

width" of the tidal-torque equilibrium rate. In effect, Peale and Gold's (1965) explanation of the 59-day spin period, although wrong, is not far wrong if the assumptions upon which Eq. (33) depends are valid.

How valid are these assumptions? As was already mentioned, the effect of varying orbital eccentricity must be analyzed. But even for fixed e, there are errors committed in passing from the original equation of motion (11) to the averaged Eq. (20). To the extent that terms of order $\beta^2$ may be neglected next to terms of order $\alpha$, our derivation is adequate. [These terms of order $\beta^2$ may arise in the solution of Eq. (11) through the "feedback" of the first order variation in $\theta$ in the term $\beta P(e, \theta, M)$.] But for Mercury it is quite possible that $\beta^2 \gtrsim \alpha$. Let us consider the possible consequences of adding a term of the form $\beta^2 F(\theta,\dot{\theta})$ to the right side of Eq. (20), in which $F(\theta,\dot{\theta})$ is some function of $\theta,\dot{\theta}$ whose absolute value is not much greater than unity for the $\theta,\dot{\theta}$ values of interest. We observe first that the positions of the equilibrium points $\theta_{eq}$ [Eqs. (25) and (26)] may be shifted slightly, by an amount of order $\beta$. This displacement compares to a previously computed displacement of order $(\alpha/\beta)$ from the positions $\theta = 0$ and $\theta = \pm\pi/2$. Such displacements are inconsequential for $\alpha << \beta << 1$. The equilibrium point near $\theta = \pm\pi/2$ must remain unstable. However, the stability of the other equilibrium point (near $\theta = 0$) is now brought into question. With $\beta^2$ terms neglected, this point was shown to be asymptotically stable for $P_k(e) > 0$ and $T_0' < 0$, with the damping rate being of order $\alpha$. Additions to this very weak damping rate of terms of order $\beta^2$ could increase it or make the equilibrium unstable. The damping of librations about the equilibrium near $\theta = 0$ is, however, intimately related to the resonance capture mechanism: in our original model it was this damping which allowed capture. Thus the discussion of capture probabilities based on perturbations of order $\alpha$ to the energy integral (27), may be rendered invalid by the presence of terms of order $\beta^2$ in the averaged equation of motion (20).

Even if the potential difficulties we have mentioned do not occur, we must still consider the possibility that the kinetic energy of the "particle" entering the "last" potential well is not uniformly distributed in an interval, but takes on certain values preferentially, resulting from the detailed dynamics implied by Eq. (11). In the next subsection, we develop an approach to the solution of (11) which answers these questions and allows us to explain adequately the spin-orbit resonance capture conditions.

C. Transformation Method

A different method of solution of Eq. (11) which leads to Eq.(20), but avoids the objections raised to simple first-order averaging, can be based on a monodromy transformation. We first rewrite (11) in the normal form

$$\left.\begin{aligned} \frac{d\theta}{dM} &= \omega \\ \frac{d\omega}{dM} &= \beta W(e,\theta,\omega,M) \end{aligned}\right\} \tag{36}$$

with

$$W(e,\theta,\omega,M) = P(e,\theta,M) + \frac{\alpha}{\beta} T(e,\omega,M) = P + \gamma T \quad , \tag{37}$$

where the functions $P(e,\theta,M)$ and $T(e,\omega,M)$ are the same as defined previously in (13) and (14), and $\gamma$ is considered to be a constant independent of $\beta$. We then assume that the solution may be expanded in a power series in $\beta$:

$$\left.\begin{aligned} \theta(M) &= \sum_{i=0}^{\infty} \beta^i \theta_i(M) \\ \omega(M) &= \sum_{i=0}^{\infty} \beta^i \omega_i(M) \end{aligned}\right\} \tag{38}$$

where

$$\theta_i(0) = \omega_i(0) = 0; \; i = 1,2,3,\ldots, \tag{39}$$

and $\theta_0(0)$ and $\omega_0(0)$ match the initial conditions. Substituting these expansions into the equations of motion and equating separately the coefficients of terms multiplied by the same power $\beta$, we obtain

$$\frac{d\theta_i}{dM} = \omega_i \quad ; \quad i = 0,1,2,... \tag{40}$$

$$\frac{d\omega_0}{dM} = 0 \tag{41}$$

$$\frac{d\omega_1}{dM} = W(e,\theta_0,\omega_0,M) \tag{42}$$

$$\frac{d\omega_2}{dM} = \theta_1(M)\left.\frac{\partial W}{\partial \theta}\right|_{\beta=0} + \omega_1(M)\left.\frac{\partial W}{\partial \omega}\right|_{\beta=0} \tag{43}$$

$$\frac{d\omega_3}{dM} = \theta_2(M)\left.\frac{\partial W}{\partial \theta}\right|_{\beta=0} + \omega_2(M)\left.\frac{\partial W}{\partial \omega}\right|_{\beta=0} + \frac{1}{2}\left[\theta_1^2(M)\frac{\partial^2 W}{\partial \theta^2} + 2\,\omega_1(M)\theta_1(M)\frac{\partial^2 W}{\partial \theta \partial \omega} + \omega_1^2(M)\frac{\partial^2 W}{\partial \omega^2}\right]\Bigg|_{\beta=0} \tag{44}$$

etc. These equations may be solved serially to obtain explicit expressions for the members $\theta_i(M)$, $\omega_i(M)$ of the power series solution (38). [The solution complete to i = 2, together with expressions for $\theta_3(M)$ and $\omega_3(M)$ for the special case of vanishing orbital eccentricity, is presented in Appendix C. The latter expressions are applicable to general spin-orbit coupling problems, e.g. the problem of Venus' spin.]

The series solution (38) provides an explicit expression for the planet's rotation angle $\theta$ and spin rate $\omega$ as a function of M and the initial conditions $\theta(0)$ and $\omega(0)$, but cannot be expected to converge for M much greater than $\beta^{-1/2}$. However we expect that over one orbital

period ($0 \leq M \leq 2\pi$) a good approximation to the exact solution is provided by the first few terms in the series. Although this expectation might be (and has been) checked by accurate numerical solutions of Eq. (36), a more general approach is possible and preferable.

Because the coefficients in the exact equation of motion are periodically time-varying, the solution may be obtained in two steps. First, the transformation is found which relates the values of $\theta$ and $\omega$ at time $M = 2\pi$ to the initial values $\theta(0)$ and $\omega(0)$. The values of $\theta$ and $\omega$ at times $M = 2n\pi$, $n = 2,3,4,\ldots$ are evidently obtained by iteration of this single-period transformation (called a monodromy transformation in differential equation theory). Second, the solution is completed in an obvious way for all time if we know $\theta(M)$ and $\omega(M)$ for $0 < M < 2\pi$ in terms of $\theta(0)$, $\omega(0)$.

Of course we need to know only the monodromy transformation exactly in order to describe the spin-orbit resonance evolution. The small fluctuations in $\theta$ and $\omega$ which occur between the times of successive perihelion passages are represented sufficiently well by one or two terms of (38) for the interpretation of observations of Mercury's rotation, and are otherwise uninteresting.

A first approximation to the exact monodromy transformation for Eq. (36) is provided by truncating (38) at $i = 1$ and setting $M = 2\pi$. We obtain (see Bellomo et al., 1967)

$$\left.\begin{aligned} \theta(2\pi) &= \theta_0(2\pi) + \beta\theta_1(2\pi) + 0(\beta^2) \\ \omega(2\pi) &= \omega_0(2\pi) + \beta\omega_1(2\pi) = 0(\beta^2) \end{aligned}\right\} , \tag{45}$$

where

$$\left.\begin{aligned} \theta_0(2\pi) &= \theta_0' + 2\pi\omega_0' \\ \omega_0(2\pi) &= \omega_0' \end{aligned}\right\} , \tag{46}$$

and

$$\theta_1(2\pi) = 2\pi^2(\alpha/\beta)T_0(e,\omega_0') + \sum_{j=-\infty}^{\infty} P_j(e)\left\{\frac{2\pi\cos 2\theta_0'}{j - 2\omega_0'} + \right.$$

$$\left. + \frac{\sin(2\theta_0' + 4\pi\omega_0') - \sin 2\theta_0'}{(j - 2\omega_0')^2}\right\} \tag{47}$$

$$\omega_1(2\pi) = 2\pi(\alpha/\beta)T_0(e,\omega_0') + \sum_{j=-\infty}^{\infty} \frac{P_j(e)}{(j-2\omega_0')}\{\cos(2\theta_0'+4\pi\omega_0')-\cos 2\theta_0'\}$$

with $\theta_0'$ and $\omega_0'$ being the initial conditions: the coefficients $P_j(e)$ are as defined in Eq. (18) and $T_0$ is the average tidal torque, defined in (16). Explicit expressions for $T_0$ are given in Appendix B. The equilibrium points, or fixed points of the monodromy transformation, are found by requiring $\theta(2\pi) = \theta_0' \pmod{\pi}$, and $\omega(2\pi) = \omega_0'$ in Eq. (45). In a linear stability analysis of these fixed points, the location in the complex plane of the pair of eigenvalues of the matrix $\underset{\sim}{J}$,

$$\underset{\sim}{J} = \begin{bmatrix} \frac{\partial\theta(2\pi)}{\partial\theta_0'} & \frac{\partial\theta(2\pi)}{\partial\omega_0'} \\ \frac{\partial\omega(2\pi)}{\partial\theta_0'} & \frac{\partial\omega(2\pi)}{\partial\omega_0'} \end{bmatrix} \tag{48}$$

is evaluated for the fixed points. It is possible to show that for $\alpha = 0$ successive values of $\theta,\omega$ at times $M = 2n\pi$, $n = 1,2,3,\ldots$, fall along curves in the $\theta,\omega$ plane corresponding to constant-value contours of the energy integral E given in Eq. (27) and derived from the averaged equation of motion (22). In general we find, as expected, that the above difference equation approach, used by Bellomo et al. (1967), and that of Goldreich and Peale (1966b), both exact to first order in $\beta$, are equivalent to this accuracy. In neither was the effect of higher-order terms in $\beta$ discussed.

In the second-order approximation to the monodromy transformation,

$$\left.\begin{aligned} \theta(2\pi) &= \theta_0(2\pi) + \beta\theta_1(2\pi) + \beta^2\theta_2(2\pi) + 0(\beta^3) \\ \omega(2\pi) &= \omega_0(2\pi) + \beta\omega_1(2\pi) + \beta^2\omega_2(2\pi) + 0(\beta^3) \end{aligned}\right\} , \tag{49}$$

we could set

$$\left.\begin{aligned} \theta(2\pi) &= \theta_0' \\ \omega(2\pi) &= \omega_0' \end{aligned}\right\} \tag{50}$$

and hope to solve the now incredibly more complicated (second-order in $\beta$) equations to find the fixed points. Then a linear stability analysis might be completed to determine the behavior of the solution in the neighborhood of these points. Fortunately following this procedure is unnecessary.

The precise locations of the fixed points near $\theta = 0$ and $\theta = \pi/2$ are unimportant. Also the libration frequency at the point near $\theta = 0$ need not be known exactly, although the complex part of this frequency, which measures the exponential damping rate of librations, must be known with an absolute error much less than $|\alpha T_0'|$. Similarly any terms in (49) representing secular accelerations of the spin must be identified if they are comparable to $\alpha T_0$. The latter two requirements are essential because the libration damping rate and the secular acceleration together determine the resonance capture probability.

Inspection of the results in Appendix C shows that the second-order terms in (49) contain no secular-acceleration terms. Only the librational damping remains to be examined. We may proceed without knowing the exact fixed-point coordinates by taking advantage of the fact that Eq. (36) represents a slightly perturbed Hamiltonian system (i.e. the monodromy transformation of the system is nearly a contact transformation). This fact is utilized in the capture probability calculation.

Following closely the development of Counselman (1968), we consider the more general single degree-of-freedom dynamic system whose equation of motion is, in Lagrangian form,

$$\frac{d}{dt}\left(\frac{\partial L}{\partial \dot{q}}\right) - \frac{\partial L}{\partial q} = f^*(q,\dot{q},t) \quad , \tag{51}$$

where $q$ is a generalized coordinate, $\dot{q} = dq/dt$, its associated generalized velocity, and $t$ the time. We assume that the Lagrangian L and the generalized force f* have an explicit periodic time-dependence:

$$\left.\begin{aligned} L(q,\dot{q},t+2\pi) &= L(q,\dot{q},t) \\ f^*(q,\dot{q},t+2\pi) &= f^*(q,\dot{q},t) \end{aligned}\right\} \tag{52}$$

for $-\infty<t<\infty$. Evidently Eq. (11) is identical with (51) if we identify

$$\left.\begin{aligned} q &= \theta \\ t &= M \\ L &= \frac{1}{2}\left(\frac{d\theta}{dM}\right)^2 + \frac{1}{2}\beta\left(\frac{1 + e\cos v}{1 - e^2}\right)^3 \cos 2(\theta - v) \\ f^* &= \alpha T(e,d\theta/dM,M) \end{aligned}\right\} \tag{53}$$

where T is the function defined in (14). It is easier, however, to work with the more general equation, (51).

If the system (51) is Hamiltonian, it is always possible to eliminate f* from the right side by including an appropriate work function in the Lagrangian. Hence we assume that f* represents only those foces not so representable. The generalized momentum $p = (\partial L/\partial \dot{q})$ and the Hamiltonian H:

$$H(q,p,t) = p\dot{q} - L \tag{54}$$

may be defined in any case and yield the pair of first-order equations

$$\left.\begin{aligned} \dot{q} &= \frac{\partial H}{\partial p} \\ \dot{p} &= -\frac{\partial H}{\partial q} + f(q,p,t) \end{aligned}\right\} \tag{55}$$

in which the function $f(q,p,t)$ replaces $f^*(q,\dot{q},t)$.

If a solution of Eqs. (55) is denoted by the 2 x 1 matrix $\underset{\sim}{x}$,

$$\underset{\sim}{x}(t) = \begin{bmatrix} q(t) \\ p(t) \end{bmatrix} , \tag{56}$$

and a neighboring solution by $\underset{\sim}{x} + \underset{\sim\sim}{\delta x}$, the deviation $\underset{\sim\sim}{\delta x}$ obeys the linear matrix differential equation

$$\frac{d}{dt} \underset{\sim\sim}{\delta x} = \underset{\sim}{A}(t) \underset{\sim\sim}{\delta x} \tag{57}$$

in which $\underset{\sim}{A}$ is the 2 x 2 matrix

$$\underset{\sim}{A}(t) = \left[\begin{array}{c|c} \dfrac{\partial^2 H}{\partial q \partial p} & \dfrac{\partial^2 H}{\partial p^2} \\ \\ -\dfrac{\partial^2 H}{\partial q^2} + \dfrac{\partial f}{\partial q} & -\dfrac{\partial^2 H}{\partial p \partial q} + \dfrac{\partial f}{\partial p} \end{array}\right] \tag{58}$$

evaluated along $\underset{\sim}{x}(t)$.

We are interested in the solution to (55) only at the times $t = 2n\pi$, $n = 0,1,2,3\ldots$, i.e. only stroboscopically. The general solution $\underset{\sim}{x}(t)$, evaluated at $t = 2\pi$, defines the monodromy transformation of (55) which maps $(q,p)$ at $t = 0$ into $(q,p)$ at $t = 2\pi$. A fixed point $(q_0,p_0)$ of this mapping evidently corresponds to a periodic solution of (55). Such periodic solutions, we have seen, characterize the spin-orbit resonance of Mercury. Two fixed points exist for each resonance, one near $(\theta,\omega) = (0,k/2)$ and the other near $(\pi/2,k/2)$ for each integer $k$. ($\theta$ is defined modulo $\pi$.) The behavior of the monodromy transformation in the neighborhood of the fixed points is determined by Eq. (57).

When the matrix $\underset{\sim}{A}(t)$ in (57) is evaluated along the periodic solution $\underset{\sim}{x}(t)$ corresponding to a stroboscopic fixed point, then Eq. (57) becomes a linear differential equation with periodic coefficients. This

type of equation is the subject of Floquet theory. It is known in this case (Counselman 1968) that the solution of (57) obeys

$$\underset{\sim}{\delta x}(2n\pi) = \underset{\sim}{J}^{n}\ \underset{\sim}{\delta x}(0) \quad ; \quad n = 0,1,2,3,... \tag{59}$$

in which $\underset{\sim}{J}$ is the 2 x 2 constant matrix defined by Eq. (48) with the elements evaluated at the fixed point. The stability of the fixed point depends on the eigenvalues of $\underset{\sim}{J}$, which must be either both real or a conjugate complex pair. The fixed point is unstable if either or both eigenvalues fall outside of a unit circle centered on the origin in the complex plane. The fixed point is asymptotically stable if both eigenvalues fall inside the unit circle. If they fall on the unit circle at angles $\pm\phi$ with respect to the real axis, then the stroboscopic values $\underset{\sim}{\delta x}$ $(2n\pi)$ are periodic samples of purely oscillatory functions of the form sin $(\phi t/2\pi)$ or cos $(\phi t/2\pi)$.

The Jacobi-Liouville formula (Cesari, 1962) relates the determinant of $\underset{\sim}{J}$ to the trace (sum of diagonal terms) of $\underset{\sim}{A}$:

$$\det \underset{\sim}{J} = \exp \int_0^{2\pi} \mathrm{tr}\ (\underset{\sim}{A})\ dt \tag{60}$$

At this point the advantage of having used a general Lagrangian formulation of the equation of motion becomes apparent: In the sum of the diagonal terms of $\underset{\sim}{A}(t)$ in Eq. (58) the mixed partial derivatives cancel, leaving simply

$$\mathrm{tr}(\underset{\sim}{A}) = \frac{\partial f}{\partial p} \tag{61}$$

Using the definitions given in (53) and substituting (61) into (60) we obtain

$$\det \underset{\sim}{J} = \exp[2\pi\alpha T_0'(e,k/2)+0(\alpha\beta)] \quad , \tag{62}$$

where $T_0'(e,k/2)$ is defined in (21). The determinant of $\underset{\sim}{J}$ is, of course, equal to the product of its eigenvalues. For the stroboscopic fixed point near $\theta = 0$ we find from Eqs. (45) to (48), but to only first order in $\beta$, that these eigenvalues lie nearly on the unit circle in the complex plane at angles of $\pm 2\pi(2\beta P_k)^{1/2}$. Eq. (62) now contributes the additional information that when $\alpha T_0' = 0$ these eigenvalues, to order $\alpha\beta$, lie <u>on</u> the unit circle. The eigenvalues are analytic functions of $\alpha$ at $\alpha = 0$. Therefore, since for Mercury $\alpha << \beta << 1$, these angles of these eigenvalues are not changed significantly when $\alpha \neq 0$. However when $\alpha T_0' < 0$ the eigenvalues must lie slightly inside the unit circle at angles near $\pm 2\pi(2\beta P_k)^{1/2}$, and their magnitudes must be almost exactly equal to $\exp(\alpha T_0' M/2)$. There is no damping effect of order $\beta^2$ and the averaged equation of motion (20) with constant coefficients represents the librational damping correctly at least to order $\alpha\beta$.

D. <u>Statistical Considerations</u>

We now demonstrate that the <u>statistical</u> properties of the solution of (12) are adequately represented by our simple model based on Eq. (20). The above results are useful for this purpose. Only the near-resonance behavior might be troublesome; i.e. only when $\omega$ is within a few "resonance widths" of the resonance rate $k/2$. Before the spin rate approaches that near to a resonance, the fluctuations in rotation are small and rapid, and the time required to decelerate from, say, 120% to 110% of the resonance rate is determined mostly by the tidal coefficient $\alpha$. Thus for the $k = 3$ resonance with $\alpha \approx 10^{-8}$ we would expect on the order of $10^7$ rotations to be completed in such a time interval, although the exact number of rotations cannot be known any better than is the value of $\alpha$. The change in $\omega$ during any <u>fixed</u> time interval $M_2 - M_1$ is similarly uncertain, and is of the order of $\Delta\alpha \cdot T_0(e,k/2)(M_2-M_1)$ where $\Delta\alpha$ represents the uncertainty in $\alpha$. For Mercury it is reasonable to consider $\alpha$ as, say, a gaussianly distributed random variable. If its standard deviation is any more than about $10^{-6}\alpha$, the two dependent random variables, $\theta \pmod{\pi}$ and $\omega$, after any reasonably large time interval, will be quite

uncorrelated because their values depend on different numbers of integrations of $d^2\theta/dM^2 \approx (\alpha T_0)$. Since $\alpha$ is not known to within even an order of magnitude, we may consider that at a time when the planet's spin approaches a resonance to within a few "resonance widths", the probability density for the spin state is nonzero and approximately uniform in a part of the $\theta$, $\omega$ plane extending in $\theta$ from $-\pi/2$ to $+\pi/2$, and in $\omega$ over an interval many times $|\pi\alpha T_0|^{1/2}$. Using this probability density in the phase plane, we can discuss the subsequent near-resonance behavior of the system in which is describable conveniently in terms of points in the phase plane. Every point in the region of non-zero probability density will follow a trajectory which either converges (stroboscopically) to the stable equilibrium point, resulting in "capture", or passes through the resonance region to "escape". Because the generalized forces are explicitly time-varying, in general three variables (e.g. $\theta$, $\omega$, and M), must be specified to completely determine its future motion. But the two variables $\theta$, $\omega$ suffice if we consider the state only stroboscopically, that is at times $M=2n\pi$ with n an integer. For simplicity when referring to motion near the kth resonance, we use the abbreviation $\dot{\theta} \equiv \omega - k/2$ for the spin rate.

The spin motion satisfying Eq. (11) generates a sequence of points $\theta$, $\dot{\theta}$ from any given initial point in the phase plane. The monodromy transformation of the differential equation maps the nth point of this sequence into the (n+1)st. These point sequences tend to fall nearly along the continuous trajectories which satisfy Eq. (23). However, we must establish that the motion of an ensemble of initial phase points, satisfying a particular probability distribution, leads to the same capture and escape probabilities as are implied by the same distribution for phase points which follow the pendulum equation (23). This may be accomplished in two steps.

First, we show that initial points distributed uniformly over a given area of the phase plane (area density $\equiv$ d) will remain uniformly distributed within their boundary for all time, as each member point is individually transformed according to the monodromy transformation.

The shape of the boundary becomes distorted, but the density of points within the area grows uniformly as the area shrinks, to the extent to which $T_0'$ is constant over that region. These properties are derived from the Jacobian of the monodromy transformation [see Eqs. (60)-(62)]. (Previously we evaluated the Jacobian only at fixed points of the transformation, but Eq. (60) and (61) are valid for any solution.) Since the derivative $T_0'$ of the tidal torque will be slowly varying, we may employ Eq. (62) for the entire region $-\pi/2 \leq \theta \leq \pi/2$ near the kth resonance $|\dot{\theta}| << 1$ and write

$$d(2\pi n) = \exp\ (-2\pi\alpha T_0'(e,k/2)n)d(0) \tag{63}$$

which relates the density of points in the "occupied" part of the phase plane after $n$ orbital revolutions to the corresponding initial density, $d(0)$. (Here we neglect that part of the argument of the exponent which is of order $\alpha\beta$.) The monodromy transformation is area-preserving only when $T_0' = 0$, in which case it is a contact transformation and (63) merely states Liouville's theorem: For a Hamiltonian system, the density of points in phase space is unchanged by the natural motion of the system. When $\alpha T_0' < 0$ the mapping reduces area by a constant ratio over the near-resonance region (i.e., where $T_0'$ remains constant). This general contraction per orbital revolution is necessary, of course, for there to be a convergence of trajectories at the stable equilibrium point near $(\theta,\dot{\theta}) = (0,0)$.

The constancy of the Jacobian allows us to derive the resonance capture probabilities very simply. We may consider the analogy between trajectories in the $\theta$, $\dot{\theta}$ plane, emanating from points uniformly distributed over some region, and streamlines of flow of a uniformly dense, uniformly contracting fluid. The particles of fluid correspond to members of the ensemble of systems whose initial conditions are uniformly distributed over some (small) region of the phase plane. Of the total flux of "fluid" passing from positive to negative $\dot{\theta}$ (actually, the flux

of ensemble members, all of whose states migrate), that fraction which converges to the stable equilibrium point is just the probability of capture for the resonance. We may compute this fraction easily after studying the phase-plane geometry shown in Fig. 2(a).

In Fig. 2(a) are drawn two trajectories, representing point sequences which converge to the unstable equilibrium point, C. [Continuous curves are drawn rather than sequences of points for convenience, but the existence of a stagnation point at C allows unique curves to be defined in any case. There are two other sequences asymptotic at C, but along which the motion is away from C (Bellomo et al. 1967).] The curves are drawn for $T_0 < 0$ and $T_0' < 0$, so that the spin rate can approach resonance only from above ($\dot{\theta} > 0$). The coordinates of C are, approximately, $(\theta,\dot{\theta}) \approx (-\pi/2 - \alpha T_0/2\beta P_k, 0)$. The stable equilibrium at $(\theta,\dot{\theta}) \approx (\alpha T_0/2\beta P_k, 0)$ is labelled D. At the unstable point C the two trajectories shown in Fig. 2(a) lie in the direction of the eigenvector of $\underset{\sim}{J}$ which corresponds to the real eigenvalue less than unity. (The other eigenvalue, real and greater than unity, corresponds to the two trajectories along which the motion is away from C.) Following the trajectories in Fig. 2(a) backward from C, we designate the points where they first cross a vertical line (constant $\theta$) through C, as A and B. For the trajectory passing through A, $\dot{\theta}$ is positive everywhere along it.

In general, the $\dot{\theta}$ coordinate of points A and B could be obtained numerically for given values of $\alpha$, $\beta$, etc., by using a computer to evaluate iteratively, but backwards in time, the expressions for the monodromy transformation, starting from initial points near C. This calculation has been done for various values of the parameters, but only as a check, because an approximate analytic solution is possible for the case of physical interest: $\alpha << \beta << 1$. We present here only the analytic solution and a remark on its accuracy, based on the numerical solutions. A manipulation of Eqs. (45) - (47) leads to the same result, to first order in $\beta$, as was derived using Eq. (20), viz.:

$$\left.\begin{aligned} \frac{1}{2}(\dot{\theta}_A)^2 &= \varepsilon+\delta \\ \frac{1}{2}(\dot{\theta}_B)^2 &= 2\delta \\ \frac{1}{2}(\dot{\theta}_C)^2 &= 0 \end{aligned}\right\} \tag{64}$$

where

$$\left.\begin{aligned} \varepsilon &= -\pi\alpha T_o(e,k/2) \\ \delta &= -2\alpha T_0'(e,k/2)(2\beta P_k(e))^{1/2} \end{aligned}\right\} . \tag{65}$$

With this result, we can calculate the capture probability simply: All of the fluid coming from the upper ($\dot{\theta} > 0$) half of the phase plane crosses the line segment ABC exactly once. The component of flow velocity perpendicular to this segment, i.e. in the $\theta$ direction, is just $\dot{\theta}$. The total flux $\phi_{AC}$ across AC is just (suppressing the uniform density):

$$\phi_{AC} = \int_0^{\dot{\theta}_A} \dot{\theta}d\dot{\theta} = \frac{1}{2}(\dot{\theta}_A)^2 \tag{66}$$

and the flux $\phi_{BC}$ across the segment BC which flows toward the stable point D and is "captured" is just

$$\phi_{BC} = \int_0^{\dot{\theta}_B} \dot{\theta}d\dot{\theta} = \frac{1}{2}(\dot{\theta}_B)^2 . \tag{67}$$

Therefore the net probability of capture at the kth resonance is

$$P_c = \frac{\phi_{BC}}{\phi_{AC}} = 2\delta/(\varepsilon+\delta) \tag{68}$$

Although we assumed for simplicity that $T_0$ and $T_0'$ were both negative near the kth resonance, the calculations for other signs of these

constants are very similar. In particular, we find Eq. (68) to be valid unless $T_0' > 0$. With the tidal torque models we have considered it impossible that $T_0' > 0$. However, variations of orbital eccentricity with time have an effect equivalent to $T_0' > 0$ under certain circumstances (see Section III). If $T_0' > 0$ the equilibrium point at D becomes unstable and librations around it have an amplitude increasing exponentially with time. In such a case if the planet's spin had been captured earlier, it would now be driven out of the resonance. [See Fig. 2(b).] The question then would be whether the planet escapes with spin faster ($\dot{\theta} > 0$) or slower ($\dot{\theta} < 0$) than the resonance rate. The calculation of the relative probabilities of these two events follows closely the lines of the derivation of Eq. (68) but with time reserved. The results are very similar. If the probabilities of escape with spin rate greater and less than the resonance rate are written as $P_e^+$ and $P_e^-$, respectively, we find that when $T_0' > 0$,

$$P_e^+ = (\delta+\varepsilon)/2\delta$$
$$P_e^- = (\delta-\varepsilon)/2\delta \quad , \tag{69}$$

where as usual the probabilities must lie in the range (0,1). Of course, $P_e^+$ will be nonzero only if $\bar{T} \equiv (T_0+T_0'\dot{\theta})$ becomes positive within the "resonance width".

Formulas (68) and (69) are strictly valid for $|\alpha T_0| \ll \beta P_k$, i.e. for the equilibrium points lying close to $\theta = 0$ and $\theta = \pi/2 (\mathrm{mod}\ \pi)$. Numerical calculations show that even for $|\alpha T_0/\beta P_k| = 0.05$, formula (68) gives probabilities $P_c$ which are too large by 0.04 when $P_c$ is about 0.5, but the relative error is less at both higher and lower values of $P_c$ and improves monotonically as $|\alpha T_0/\beta P_k|$ approaches zero. For the treatment of Mercury's spin-orbit resonances, formulas (68) and (69) are perfectly adequate.

## III. VARIATIONS IN ORBITAL ECCENTRICITY

### A. Orbit Perturbations

So far we have considered Mercury's orbit to be a fixed ellipse. In fact, all of Mercury's orbital elements vary because of perturbations by the other planets. (The well-known effects attributed to general relativity are insignificant here.) Unfortunately the current state of development of celestial mechanics, and of planetary theory in particular, allows us to say nothing with certainty about Mercury's orbit at times as remote as $10^9$ years ago. Even the basic question of the stability of the solar system over such a time interval remains open (see, e.g., Hagihara, 1961). Perhaps the best estimate, really a guess (Brouwer and Clemence, 1961), of the very-long-term behavior of planetary orbits is provided by the "secular" variations which, by definition, are those computed by limiting the planetary disturbing function to the part independent of the mean longitudes. In the first-order solution of the planetary n-body problem by expansion in powers of the disturbing masses there are in general both secular terms and periodic terms. Because the spin-orbit resonance mechanism effectively averages over many orbits, the periodic orbital variations are unimportant. (An exception would occur if Mercury were involved in an orbital resonance with one or more other planets.)

This method of secular perturbations has been applied to the planets Mercury through Neptune by Brouwer and van Woerkom (1950), who refined it to include the principal effect of the great inequality between Jupiter and Saturn. The typical solution for the eccentricity $e_\alpha$ and longitude of perihelion $\pi_\alpha$, measured from a fixed direction in inertial space for the planet $\alpha(\alpha = 1,2,\ldots,8)$, is of the form

$$Z_\alpha = \sum_{k=1}^{10} N_{\alpha k} \exp\,(i\phi_k - is_k t) \tag{70}$$

$$|Z_\alpha| \equiv e_\alpha' \equiv 2 \sin\left(\frac{1}{2}\sin^{-1} e_\alpha\right) \underset{e_\alpha \to 0}{\approx} e_\alpha$$

$$\pi_\alpha \equiv \text{Arg } Z_\alpha$$

where $i \equiv \sqrt{-1}$, and $N_{\alpha k}, \phi_k$, $s_k$ are real constants ($\underline{k}$ ranges from 1 to 10 because of the inclusion of the great inequality).

A very similar expression, yielding the inclinations $\gamma_\alpha$ and longitudes $\theta_\alpha$ of the ascending nodes (both referred to the invariable plane) is obtained by replacing $e_\alpha'$ by $\sin \gamma_\alpha$ and $\pi_\alpha$ by $\theta_\alpha$ in Eqs. (70). A different set of constants $I_{\alpha k}$ and $\psi_k$ replace $N_{\alpha k}$, $\phi_k$ in this case. The circular frequencies $s_k$ appearing in (70) are determined by the planetary masses and semi-major axes, which remain constant. The present values of the eccentricities, perihelia, inclinations, and nodes serve to determine the constants of integration $N_{\alpha k}$, $\phi_k$, $I_{\alpha k}$, and $\psi_k$. The values obtained by Brouwer and van Woerkom for $\phi_k$, $s_k$, and $N_{1k}$ ($\alpha = 1$ for Mercury) are listed in Table 1.

The inclination to the invariable plane of Mercury's orbit according to this theory will never exceed the sum of all the $I_{1k}$. This limit is less than 10°, so that we shall here ignore variations of the orbital plane. (However, in a study of the evolution with time of the axis direction, the motion of the plane and the "ability" of the spin axis to follow it must be analyzed.) Also unimportant are the uniform and accelerated motion of the sun-perihelion reference line, measured by the rate of advance of $\pi_1$. The uniform part of the advance does not play an important role. Only minor modifications are required: One may consider the anomalistic period as basic and modify the equilibrium points accordingly, taking into account the difference in (inertial) orientation after each period. The accelerated part of the advance is very small and also of no concern. Since $N_{11} \approx 0.175$ and

$$\sum_{k=2}^{10} |N_{1k}| \approx 0.066,$$

a good approximation to the greatest possible magnitude of $d^2\pi_1/dM^2$ is given by

$$\max \left| \frac{d^2\pi_1}{dM^2} \right| \simeq n^{-2} N_{11}^{-1} \sum_{k=1}^{10} |N_{1k}| (s_1 - s_k)^2 , \tag{71}$$

where $n$ is Mercury's orbital mean motion given in the same units as $s_k$. Substitution of numerical values from Table 1 yields

$$\max \left| \frac{d^2\pi_1}{dM^2} \right| \simeq 2 \times 10^{-13} \tag{72}$$

which is more than three orders of magnitude smaller than the acceleration due to the tidal torque alone when the tidal parameter $\alpha = 10^{-9}$.

Because the value and rate of change of Mercury's orbital eccentricity in particular are crucial to the spin-orbit resonance phenomena, we must know the behavior of this element during Mercury's past orbital history in order to study properly these resonances. The time dependence of $e$ is given by

$$e(t) \simeq e_1' = \left| \sum_{k=1}^{10} N_{1k} \exp (i\phi_k - is_k t) \right| \tag{73}$$

Part of this function is shown in Fig. 3(a). From the figure, or from the coefficients in Table 1, it is evident that the behavior of e(t) is dominated by three terms: $N_{11}$, $N_{12}$, and $N_{15}$. Physically, this result follows from Venus and Jupiter being the dominant planets in their perturbing effect on Mercury. Because $N_{11}$ is much greater than the other coefficients, the eccentricity has an average value nearly equal to $N_{11}$, and exhibits two superimposed nearly-sinusoidal oscillations of amplitudes $N_{12}$ and $N_{15}$ with frequencies $(s_1-s_2)$ and $(s_5-s_1)$, respectively. The other seven terms in the sum in (73) contribute fairly small oscillations of various periods.

The two frequencies $(s_1-s_2)$ and $(s_5-s_1)$ are nearly commensurable in the ratio 8:5. In about $5.5 \times 10^6$ years the argument involving $(s_1-s_2)$ completes 8 cycles and that for $(s_5-s_1)$ completes 5. The

deviation from exact commensurability is about one per cent of the period of the former so that in about 70 x $10^6$ years the interference pattern generated between the two terms repeats itself. However because of the fairly high order of 8:5 commensurability, a section of length 5.5 x $10^6$ years taken from the e(t) "waveform" looks about the same regardless of its position in the 70 x $10^6$ year interference period. For practical purposes, therefore, the eccentricity may be approximated by the periodic function,

$$e(t) = e_0 + \sum_{k=1}^{\ell} e_k \sin[2\pi\, n_k(t/\tau_e)+\kappa_k] \ , \tag{74}$$

where $\tau_e$ is the period and the $n_k$ are integers. A six-frequency approximation to (73), generated by taking $e_i = N_{1,i+1} (i = 0 \to 6)$, $\tau_e$ = 5.52 x $10^6$ years, $n_k (k = 1 \to 6)$ = 8, 50, 53, 5, 95, 11, with all the $\kappa_k$ = 0, except $\kappa_1 = 194^\circ.70$ and $\kappa_4 = 152^\circ.63$, is plotted in Fig. 3(b). This periodic eccentricity function has been used in the computation of the Mercury spin-orbit resonance capture probabilities according to the method described below. It has also been found that no significant change in these probabilities occurs when the six-frequency function is replaced with the much simpler and smoother function obtained by taking $\ell = 2$ in (74), with $e_0 = N_{11}$, $e_1 = N_{12}$, $e_2 = N_{15}$, and $n_1 = 8$, $n_2 = 5$, preserving the same period $\tau_e$. It is reassuring that the small details of eccentricity behavior are insignificant.

B. Spin Equation of Motion with Varying Eccentricity

From the preceding we see that the orbital eccentricity change during one orbital period is small, so that the derivation of the averaged spin equation of motion (30) from the original equation (20), which is time-varying with orbital period, remains valid. We have

$$\ddot{\theta} + \beta P_k(e) \sin 2\theta = \alpha T_0(e) + \alpha T_0'(e)\dot{\theta} \tag{76}$$

in which the coefficients $P_k(e)$, $T_0(e)$, and $T_0'(e)$ are now considered to be slowly varying. As a result we will find that multiple captures and escapes may occur at the same spin-orbit resonance. For example, during a time when the orbital eccentricity is essentially stationary at a sufficiently high value, the planet's spin rate might be decelerated by the tidal torque and be captured in a resonance, as described in Section II. Librations of the instantaneous spin rate might then decay. If the orbital eccentricity now begins to decrease, however, the amplitude of librations about the resonance spin rate may actually grow, through adiabatic "pumping", as the coefficient $P_k(e)$ decreases. Eventually the librations may grow so large that the spin motion ceases to be libratory with respect to the resonance rate, and becomes circulatory. The direction of the circulatory motion might be in either sense with respect to the resonance. If the relative spin becomes circulatory in the positive sense (actual spin rate faster than resonance rate), then certainly at some future time as the rate of eccentricity decrease diminishes the spin will again be slowed to resonance. At such a time capture might again take place, or passage through the resonance to slower spin might occur. In order to calculate the probability of permanent, ultimate capture in a given resonance, it is necessary to consider each possible temporary capture, to consider the possibilities of escape following a capture, and so on, combining these probabilities in the end to find the overall probability of the compound event. Because each of these probabilities is now periodically time-varying (i.e. a function of phase within a cycle of eccentricity variation), a method will be needed to determine the times of possible captures or escapes (when the actual spin rate reaches resonance, or the stroboscopic rate $\dot{\theta}$ reaches zero).

The overall probability of ultimate capture is calculated by considering an initial set of systems with initial conditions uniformly distributed at a given epoch over an area in phase space somewhat above the resonance region. (We are here discussing the probability of capture into a particular resonance state on the assumption that all higher

resonances have already been passed.) For any initial epoch the probability of ultimate capture for a (randomly chosen) member of the initial set may be calculated by repeated partitioning and recombining of the original set: We begin by computing the probability of "temporary" capture at the original epoch. We adopt the notation $P\{C';t_0\}$ for this probability, where $t_0$ is the initial epoch and C denotes capture, with the prime signifying "temporary". The original set of systems would thus be divided into two subsets with the probabilities of a randomly chosen member belonging to the temporarily captured, or temporarily escaping subset, being given by (respectively) $P\{C';t_0\}$ or $1-P\{C';t_0\}$. Next, a (randomly selected) system from each of the two subsets may be considered. For example, the evolution of a system temporarily captured (first subset) is followed using the equation of motion (derived below) to determine the time (if any) of a possible escape - to either faster or slower spin. The conditional probabilities $P\{E_+';\ t_1|C';\ t_0\}$ and $P\{E_-';t_1|C';t_0\}$ - for temporary escape to faster ($E_+'$) and slower ($E_-'$) spins at time $t_1$ following temporary capture at time $t_0$ - are then calculated and the first subset with associated probability $P\{C';t_0\}$ is partitioned accordingly. The time interval between successive capture and escape opportunities is in general so great compared to the libration period that we may safely assume that each system has lost all "memory" of its state at the time of an earlier capture. We are able, therefore, to use unconditional probability formulae such as were derived in Section II.D for subdividing the various subsets at times of possible captures and escapes. The calculation of probabilities and subdivision of sets proceeds in this manner with each alternate path being followed until permanent capture or permanent escape occurs. (The criteria for these two terminal events will be discussed below.) The overall probability of ultimate capture $P\{C;t_0\}$ for a member of the starting set of systems is then obtained by recombining the subsets (adding their associated probabilities) which reached permanent capture. The overall probability $P\{C;t_0\}$ will be given by a sum of cascaded products of the type $P\{C';t_n|E_-';t_{n-1}\}\cdot P\{E_-';t_{n-1}|C';t_{n-2}\}$ $\ldots P\{C';t_0\}$. Although the number of branches or subdivisions of the

original set might in principle be enormous, in practice with physically reasonable values of $\alpha$ and $\beta$ the number of branches is small, or the probability calculation can be stopped at a point where the fraction of the original set whose ultimate fate remains undecided falls below a small, arbitrary threshold.

The probability of ultimate capture $P\{C;t_0\}$ so far determined still depends on the initial epoch, $t_0$. We must therefore ask: is the spin rate equally likely to reach resonance at all times, $t_0$; or, since the eccentricity variation is quasi-periodic, at all phases within a cycle? In fact all phases will not be equally likely; it may even be impossible for the spin rate to reach resonance at certain phases, for reasons discussed below. It will be found, however, that only a few "resonance widths" above resonance [$\omega_\beta \equiv (2\beta P_k)^{1/2}$ is the "resonance width"] the distribution of arrival times becomes essentially uniform in phase. It becomes possible, therefore, to average the computed capture probabilities over one cycle in $t_0$, provided that the spin evolution and probability calculation is started beyond a few times $\omega_\beta$ above resonance.

In order to follow the near-resonance spin motion when eccentricity is variable, we will use a normalized energy function $E_n$ of $\theta$, $\dot{\theta}$, and e, which is obtained by simply dividing the energy function E (Equation 33) by the square of the (now time-varying) resonance width (Equation 39):

$$E_n(\theta,\dot{\theta},e) = \frac{1}{2}(\dot{\theta})^2(2\beta P_k(e))^{-1} - \frac{1}{2}\cos^2\theta \tag{78}$$

In general the time derivative $dE_n/dM \equiv \dot{E}_n$ is [using Equation (76)]

$$\dot{E}_n = [\tfrac{1}{2}(\dot{\theta})^2(2\beta P_k)^{-1}]\cdot[2\alpha T_0' - (\dot{P}_k/P_k)]$$

$$+ [\dot{\theta}(2\beta P_k)^{-1/2}]\cdot[\alpha T_0 \cdot (2\beta P_k)^{-1/2}] \tag{79}$$

where

$$\dot{P}_k \equiv dP_k/dM = (dP_k/de)(de/dM). \tag{80}$$

Evidently if $\alpha = 0$ and $\dot{e} \equiv de/dM = 0$ then (as expected) $\dot{E}_n$ is identically zero and $E_n$ is an integral of the motion. Contours of constant $E_n$ may be drawn in the $\theta,\dot{\theta}$ plane, and these must coincide with phase trajectories of Equation (76) when $\dot{E}_n=0$. Examples of such contours are shown in Fig. 4. The special contour defined by $E_n=0$ is called the separatrix because it separates the two regions of circulating trajectories ($E_n > 0$ with either $\dot{\theta} > 0$ or $\dot{\theta} < 0$ from the interior region of librating trajectories ($-1/2 < E_n < 0$).

We are not so much concerned with knowing Mercury's actual spin state, as with knowing the changes in the value of $E_n$, because the times when $E_n = 0$ are times of possible capture or escape events. When $E_n > 0$, the planet is "outside" the resonance region; under the combined influences of the tidal torque and eccentricity variation [through $\dot{P}_k$ in Eq. (79)], $E_n$ may slowly be reduced until it reaches zero. At that time there is in general some probability that the spin will be "captured" in the resonance (i.e., that $E_n$ will go negative), and a complementary probability that the spin state will pass through the resonance (i.e, that $\dot{\theta}$ will change sign and $E_n$ stay positive). The probability formulas derived earlier for these events will of course have to be modified to include the effect of eccentricity variations. With appropriate probability formulas to treat the situations when $E_n$ reaches zero (from both positive and negative $\dot{\theta}$), and with a differential equation to describe the time variation of $E_n$, we can determine the probability of ultimate capture in a resonance as described above, by combining the probabilities for the individual events.

Eq. (79) is a differential equation describing the time dependence of $E_n$, but (79) cannot be integrated directly because the right side depends on $\dot{\theta}$ which is not uniquely determined by the values of $E_n$ and the time. [By the same token, of course, Eq. (78) is not of direct use since it does not give $E_n$ explicitly as a function of time.] Because $\alpha << \beta$ and $\dot{P}_k(e) << 1$, the energy function $E_n$ will change only slowly with time so that over moderately long time intervals the (stroboscopic) spin state will follow closely a contour of constant $E_n$ in the phase plane. Thus, for libration ($E_n < 0$) when the amplitude is not large,

the period is approximately $2\pi(2\beta P_k)^{-1/2}$, whereas $\dot{E}_n$ is of the order of $\alpha\beta^{-1/2}$, so that the change of $E_n$ during one libration period is of the order of $\alpha\beta^{-1}$, which for Mercury is small compared to unity. A similar argument applies for circulation ($E_n > 0$) unless $E_n$ is very small, i.e. unless the circulating trajectory passes very near the unstable fixed point at $(\theta,\dot{\theta}) \approx (-\frac{\pi}{2},0)$. In order to apply the theory of capture probability developed in Section II, however, we must show that the times spent on phase trajectories which do pass near the unstable equilibrium point [C in Fig. 2(a)] may be neglected in comparison with the period of eccentricity variation.

The influence of the unstable point causes libration and circulation periods to diverge as $E_n \to 0$:

$$\left.\begin{aligned} T_{circ} &\underset{E_n\to 0}{\to} -(2\beta P_k)^{-1/2} \ln E_n \\ T_{lib} &\underset{E_n\to 0}{\to} -2(2\beta P_k)^{-1/2} \ln |E_n| \end{aligned}\right\} \qquad (81)$$

[The second of Eqs. (81) yields a period twice as large as the first near $E_n = 0$ because, by definition, the libration period extends over a "round-trip" in the phase strip whereas the circulation period is only a "one-way" affair.] Does this divergence of periods cause any difficulties? From Fig. 2(a) we see that as a system enters the resonance region from above ($\dot{\theta} > 0$), its trajectory must pass between points A and C. Only an entirely negligible fraction of an ensemble of systems with randomly chosen initial conditions will enter the resonance region with an energy sufficiently near zero to have a circulation or libration period comparable to or greater than that of the eccentricity variation. This statement is easily proved: from Eqs. (64), (65), (78) and a simple calculation of the change in $E_n$ attributable to $\dot{P}_k$ during one circulation cycle, we find

$$E_n(A) = \left|-\pi\alpha T_0/(2\beta P_k)+[(\dot{P}_k/P_k)-2\alpha T_0']/(2\beta P_k)^{1/2}\right| , \tag{82}$$

which is of order $\alpha/\beta$ and would be about $10^{-5}$ for Mercury if $\alpha \approx 10^{-9}$ and $\beta \approx 10^{-4}$. (The term $\dot{P}_k/P_k$, being variable, could lead to cancellations but these would certainly be so infrequent as to be quite negligible.) Even a trajectory for which $E_n$ equals $10^{-8}$ passing point A, will, according to Eq. (81), have a circulation period of only about 500 yr (for $2\beta P_k \approx 10^{-4}$) - negligible compared with the period of eccentricity variation. Since, for this case, only about 1 in $10^6$ members of the ensemble will have a trajectory passing between A and C with $E_n \leq 10^{-8}$, our conclusion is established.

We now return to the problem of integrating Eq. (79). Since neither $E_n$ nor $P_k$ will change appreciably during a libration or circulation period, we may replace the quantities $[\frac{1}{2}(\dot{\theta})^2(2\beta P_k)^{-1}]$ and $[\dot{\theta}(2\beta P_k)^{-1/2}]$ by their average values over such a period. Thus, for $E_n > 0$,

$$\left\langle \tfrac{1}{2}\dot{\theta}^2(2\beta P_k)^{-1} \right\rangle \equiv \frac{1}{T_{circ}} \int_0^{T_{circ}} \tfrac{1}{2}\dot{\theta}^2(2\beta P_k)^{-1} dM$$

$$= \frac{1}{T_{circ}} \int_{-\pi/2}^{\pi/2} \tfrac{1}{2}|\dot{\theta}|(2\beta P_k)^{-1} d\theta \tag{83}$$

where we have used $dM = d\theta/\dot{\theta}$. Substituting for $\dot{\theta}$ from Eq. (78) and rearranging, we obtain

$$\left\langle \tfrac{1}{2}\dot{\theta}^2(2\beta P_k)^{-1} \right\rangle = \frac{L(\mu)}{\mu T_{circ}(2\beta P_k)^{1/2}} \; ; \; \mu \equiv (2E_n+1)^{-1/2} \tag{84}$$

where

$$L(\mu) \equiv \int_0^{\pi/2} [1-\mu^2\sin^2\theta]^{1/2} d\theta \tag{85}$$

is the complete elliptic integral of the second kind. For $T_{circ}$, we have

$$\left.\begin{aligned} T_{circ} &\equiv \int_0^{T_{circ}} dM = \int_{-\pi/2}^{\pi/2} \frac{d\theta}{|\dot{\theta}|} = 2\mu K(\mu)(2\beta P_k)^{-1/2} ; \\ \mu &\equiv (2E_n+1)^{-1/2} \end{aligned}\right\} \tag{86}$$

where

$$K(\mu) \equiv \int_0^{\pi/2} [1-\mu^2\sin^2\theta]^{-1/2} d\theta \tag{87}$$

is the complete elliptic integral of the first kind. Eqs. (84) and (86) yield, of course

$$\left\langle \frac{1}{2}\dot{\theta}^2(2\beta P_k)^{-1} \right\rangle = \frac{L(\mu)}{2\mu^2 K(\mu)} ; \qquad E_n > 0 ; \tag{88}$$

similarly, we find

$$\left\langle \dot{\theta}(2\beta P_k)^{-1/2} \right\rangle = \frac{\pm\pi}{2\mu K(\mu)} ; \quad E_n > 0 , \tag{89}$$

where the plus sign is valid for the region above the resonance ($\dot{\theta} > 0$), and the minus sign holds for below ($\dot{\theta} < 0$).

Defining

$$\left.\begin{aligned} \delta(M) &\equiv -2\alpha T_0' + \dot{P}_k/P_k \\ \varepsilon(M) &\equiv -\pi\alpha T_0/(2\beta P_k)^{1/2} \end{aligned}\right\} \tag{90}$$

in analogy with Eq. (65), we may now replace Eq. (79) by

$$\dot{E}_n = -[2\mu K(\mu)]^{-1}[\mu^{-1}L(\mu)\delta(M) \pm \varepsilon(M)]; \qquad E_n > 0 , \tag{79a}$$

where the right side has been averaged over a circulation period. The M-dependence of $\delta$ and $\epsilon$ follows from that of $P_k$, $T_0$, and $T_0'$.

Inside the resonance region ($E_n < 0$), we find

$$\left\langle \frac{1}{2}\ \dot{\theta}^2(2\beta P_k)^{-1} \right\rangle = \frac{1}{T_{lib}} \int_0^{T_{lib}} \frac{1}{2}\dot{\theta}^2(2\beta P_k)^{-1} dM$$

$$= \frac{1}{T_{lib}} \int_{-\theta_1}^{\theta_1} |\dot{\theta}|\ (2\beta P_k)^{-1} d\theta \qquad (91)$$

where

$$\theta_1 \equiv \sin^{-1}(1+2E_n)^{1/2} \quad ; \quad -\frac{1}{2} < E_n < 0 \qquad (92)$$

is the libration amplitude. Using Eq. (78) and the well-known integral (see, for example, Gradshteyn and Ryzhik, 1965):

$$\int_0^{\pi/2} \frac{\cos^2 x\ dx}{(1-\mu^{-2}\sin^2 x)^{1/2}} = \mu^2 L(\mu^{-1}) + (1-\mu^2)K(\mu^{-1}) \quad , \qquad (93)$$

in combination with the change of variables $\sin x = (2E_n+1)^{-1/2} \sin\theta$, yields

$$\left\langle \frac{1}{2}\dot{\theta}^2(2\beta P_k)^{-1} \right\rangle = E_n + L(\mu^{-1})[2K(\mu^{-1})]^{-1};$$

$$\mu^{-1} = (2E_n+1)^{1/2} \quad ; \quad E_n < 0, \qquad (94)$$

where we have used, in addition, the expression for $T_{lib}$:

$$T_{lib} \equiv \int_0^{T_{lib}} dM = 2\int_{-\theta_1}^{\theta_1} \frac{d\theta}{|\dot{\theta}|} = 4(2\beta P_k)^{-1/2} K(\mu^{-1}) \quad . \qquad (95)$$

Since for $E_n < 0$ the analog of Eq. (89) vanishes (in our approximation the libration cycle is taken to be symmetric, therefore yielding a zero average value for $\dot{\theta}$), we obtain

$$\dot{E}_n = -\{E_n + L(\mu^{-1})[2K(\mu^{-1})]^{-1}\}\delta(M) \; ; \; \mu^{-1} = (2E_n+1)^{1/2} \; ; \; E_n<0 \; . \qquad (79b)$$

The right sides of Eqs. (79a) and (79b) depend only on M, hence these equations may be integrated numerically to determine the time that $E_n$ reaches zero, given any initial value of $E_{n0}$ at an initial time $M_0$. No difficulty is caused by the divergence of $K(\mu)$ as $\mu \to 1 (E_n \to 0)$; the singularity is analytically integrable. Since Eq. (79b) is separable, it is easier to use a new function $F_n$ for motion inside the separatrix where we define $F_n = 0$ when $E_n = 0$ and

$$dF_n = \{E_n + L(\mu^{-1})[2K(\mu^{-1})]^{-1}\}^{-1} dE_n \; . \qquad (96)$$

Thus

$$\frac{dF_n}{dM} = -\delta(M) \qquad (97)$$

which may be solved by quadrature to follow the spin evolution inside the separatrix, in particular to find the later time, if any, of escape from a resonance following capture. When the orbital eccentricity is a periodic function of time as in Eq. (75), then so is the function $\delta(M)$. For convenience in the numerical work, we separate $\delta(M)$ into two parts: its average value $\langle \delta(M) \rangle$ and the periodic variation $\delta_p(M)$ about $\langle \delta(M) \rangle$ .

Because $T_0'(e) \leq 0$ for all e, it is evident from Eq. (90) that $\langle \delta(M) \rangle$ must be non-negative. It will also be useful to define the definite integral $I_p(M)$ of $\delta_p(M)$:

$$I_p(M) \equiv \int_0^M \delta_p(M')dM' = \int_0^M (\delta(M') - \langle \delta \rangle)dM' \qquad (98)$$

Note that $I_p(\tau_e) = I_p(0) = 0$, where $\tau_e$ is the period of the eccentricity variation. This integral $I_p(M)$ may be tabulated in advance for one eccentricity period $\tau_e$, and the table may be used to find the time the spin state again reaches the separatrix following a (temporary) capture. We thus avoid numerical integration, requiring quadrature only once for given functions $T_0'(e)$, $P_k(e)$, and $e(M)$. At the instant of capture, defined as $M = M_c$, we have $F_n = 0$, with $\dot{F}_n < 0$. From Eqs. (97) and (98) we have, for $M > M_c$,

$$F_n(M) = -(M-M_c)\langle\delta\rangle - I_p(M)+I_p(M_c) \tag{99}$$

which is valid as long as $F_n$ remains negative. Escape from the separatrix occurs when $F_n = 0$ with $\dot{F}_n > 0$, i.e. at the earliest time $M_1$ in the interval $M_c < M_1 < M_c+\tau_e$ for which the condition

$$I_p(M_1) \leq I_p(M_c) - \langle\delta\rangle (M_c-M_1) \tag{100}$$

is satisfied. Since $\langle\delta\rangle$ and $M_c$ are known, we need only refer to the table of $I_p(M)$ vs. M, using interpolation as required, in order to determine the escape time $M_1$. The value of $M_1$ modulo $\tau_e$, of course, is the tabular argument. Because $I_p(M)$ has period $\tau_e$, and because the coefficient $\langle\delta\rangle$ of $M_1$ in the right side of inequality (100) is positive, it follows that if no solution $M_1$ lies in the interval $M_c < M_1 < M_c+\tau_e$, then none exists for larger $M_1$ and the capture is permanent.

The probability formulae required for the moment when $E_n$ reaches zero from above (possible capture) or below (escape possible with either sign of $\dot{\theta}$) are given by Eq. (68) and (69), where the functions $\delta$ and $\varepsilon$ must be evaluated at the time $E_n = 0$ according to Eq. (90).

The theory needed to predict the ultimate fate of an ensemble of systems which have initial energies spread near $E_{n0}$ at time $M_0$ is now completely developed. We review the procedure, which has been programmed for a digital computer. Eq. (79a) is integrated numerically

from the given initial condition until $E_n = 0$ is reached. A step size of a few thousand years is appropriate. The functions $\delta(M)$ and $\varepsilon(M)$ are tabulated in advance, as is the quantity $[2\mu K(\mu)]^{-1}$ which is a function only of $E_n$. The end time having been determined, the initial ensemble is divided into two parts according to the capture probability formula (68). The fraction which penetrates the resonance is "followed" again by numerical integration of Eq. (79a), with the opposite sign now used for $\varepsilon(M)$. If this fraction fails to return (within one eccentricity period) to the $E_n = 0$ state, it is recorded as having permanently avoided capture at the resonance. If it returns to $E_n = 0$ again, it is treated in the same manner as was the initial ensemble. That fraction of the systems captured when $E_n$ first reaches zero will be further divided if Inequality (100) is satisfied at some time during the eccentricity cycle. At such a time the probability formula (69) is used to partition these systems into two classes: those that pass outside the separatrix with $\dot{\theta} > 0$ and those that leave with $\dot{\theta} < 0$. The two classes are each followed by the use of Eq. (79a) and ultimately disposed of in the manner already described.

This algorithm has been programmed for an IBM 360/65 digital computer following the description we have given. Because an arbitrarily large initial ensemble may be divided in two in principle many times, one might imagine the embarrassing result occurring that a veritable aerosol of subensembles is obtained, the algorithm never terminating. For the range of parameters believed appropriate for Mercury, no difficulty has occurred because before a dozen subensembles have been produced that fraction of the systems either permanently captured or permanently lost approaches 99.9% of the total. After a few seconds have been spent for the tabulation of the various functions required, typically less than one second of central-processor time is required to completely dispose of an ensemble of systems whose initial states lie five to ten "resonance widths" above a resonance, with values of $\alpha$, $\beta$ corresponding, respectively, to tidal-effective-Q's varying from 10 to 500, and planetary (B-A)/C varying from $10^{-4}$ to $10^{-6}$.

Two additional parameters must be considered before the total probability of (ultimate) capture at a resonance can be calculated for a given $\alpha$, $\beta$ and choice of tidal model: the initial value of $E_n$ and the initial time. These are easily treated by (1) considering a range of initial times distributed over an eccentricity cycle; and (2) observing that the resultant probabilities become <u>independent</u> of the starting value of $E_n$ when it exceeds about 25 for $\alpha$ and $\beta$ lying in the ranges given above. (Recall that a value of $E_n = 25$ corresponds to $\dot{\theta} \simeq \pm 7\omega_\beta \equiv \pm 7\sqrt{2\beta P_k}$, i.e. to an actual spin period only a few per cent more than the resonance value.) The use of initial times distributed over an eccentricity period $\tau_e$ does not constitute a Monte Carlo experiment. The capture probability, determined by the fraction of the initial ensemble captured permanently, is a well-defined function of the initial time. The average probability, defined by the integral over a range of initial times (corresponding to an eccentricity cycle), is approximated, for example, by the use of a number of uniformly spaced initial times. The number required for a given accuracy depends on the smoothness of the probability as a function of initial time. In the limit of constant eccentricity only one sample need be computed, and the present method reduces to that described in Section II.

## IV. CORE MANTLE COUPLING

The theory developed in the preceding section is easily modified to include a simple core-mantle coupling of the type considered by Goldreich and Peale (1967) in an ingenious attempt to explain the control apparently exerted by the earth on Venus' spin. We will use the same simple model in which a rigid axially-symmetric core is coupled to a concentric outer shell (mantle) be a torque linear in the relative angular velocities. We denote the core angular velocity by $\dot{\eta}$, and take the core-mantle torque proportional to the difference $(\dot{\theta}-\dot{\eta})$ such that the exponential relaxation time for this angular velocity difference is $\sigma^{-1}$. If $\sigma \ll 1$ and with the ratio of the core moment-of-inertia to that of the mantle denoted by $\rho$, we may derive averaged equations analogous to Eq. (20):

$$\ddot{\theta} + \beta P_k \sin 2\theta = \alpha T_0 + \alpha T_0' \dot{\theta} - \rho\sigma(\dot{\theta} - \dot{\eta}) \tag{101}$$

for the mantle and

$$\ddot{\eta} + \sigma\dot{\eta} = \sigma\dot{\theta} \tag{102}$$

for the core where all quantities are defined in analogy with the uses in prior sections; for example

$$\beta \equiv \frac{3}{2}\left[\frac{(B-A)}{C}\right]_{\text{mantle}} \tag{103}$$

and

$$\alpha T_0 = \langle \text{tidal torque} \rangle / n^2 C_{\text{mantle}} \quad . \tag{104}$$

We define a new variable $\dot{\zeta}$ to describe the core angular velocity:

$$\dot{\zeta} = \frac{\pi}{2}\dot{\eta}(2\beta P_k)^{-1/2} \quad ; \tag{105}$$

in terms of this variable, the time derivative of $E_n$, defined in Eq. (78), becomes

$$\dot{E}_n = \left[\frac{1}{2}(\dot{\theta})^2(2\beta P_k)^{-1}\right]\cdot\left[2\alpha T_0' - (\dot{P}_k/P_k) - (2\rho\sigma)\right] + \left[\dot{\theta}\pi^{-1}(2\beta P_k)^{-1/2}\right]\cdot\left[\pi\alpha T_0(2\beta P_k)^{-1/2} + (2\rho\sigma)\dot{\zeta}\right] \quad . \tag{106}$$

The derivative of $\dot{\zeta}$ satisfies

$$\ddot{\zeta} = \sigma\cdot\left[\frac{\pi^2}{2}(\dot{\theta}\pi^{-1}(2\beta P_k)^{-1/2}) - \dot{\zeta}\right] - \frac{1}{2}(\dot{P}_k/P_k)\dot{\zeta} \quad . \tag{107}$$

If $\sigma^2 << \beta$ and $\alpha << \beta$ we may average the $\dot{\theta}$-dependent quantities on the right sides of Eqs. (106) and (107) over a libration or circulation period of $\theta$, keeping $E_n$ constant as in the previous section. Defining the averages $g(E_n)$ and $h(E_n)$:

$$\left.\begin{aligned} g(E_n) &\equiv \left\langle \frac{1}{2}(\dot{\theta})^2(2\beta P_k)^{-1} \right\rangle \\ h(E_n) &\equiv \left\langle \dot{\theta}\pi^{-1}(2\beta P_k)^{-1/2} \right\rangle \end{aligned}\right\} \tag{108}$$

which were computed in Section III, we obtain

$$\ddot{\zeta} = \sigma\cdot\left[\frac{\pi^2}{2}h(E_n) - \dot{\zeta}\right] - \gamma(M)\dot{\zeta} \tag{109}$$

$$\dot{E}_n = h(E_n)\cdot\left[-\varepsilon(M) + (2\rho\sigma)\dot{\zeta}\right] - g(E_n)\cdot\left[\delta(M) + (2\rho\sigma)\right] \tag{110}$$

where

$$\gamma(M) \equiv \frac{1}{2}(\dot{P}_k/P_k) \quad . \tag{111}$$

The pair of equations, (109) and (110), replaces Eq. (79a). In the probability formulae (68) and (69) it is necessary only to replace the quantity $\varepsilon$ by $\varepsilon - (2\rho\sigma)\dot{\zeta}$ and the quantity $\delta$ by $\delta + 2\rho\sigma$. With these changes the

algorithm developed in Section III may be applied as before. As mentioned there certain simplifications are possible when $E_n$ is negative: numerical integration of (79b) was not required in this region. Similar simplifications remain available with the pair (109) and (110). When $E_n < 0$, these equations become uncoupled:

$$\left.\begin{aligned} \ddot{\zeta} &= -[\gamma(M)+\sigma]\cdot\dot{\zeta} \\ \dot{E}_n &= -g(E_n)\cdot[\delta(M)+2\rho\sigma] \end{aligned}\right\} \quad ; \qquad E_n < 0 \ . \tag{112}$$

In direct analogy with Eq. (97) we define $F_n$ such that

$$\frac{dF_n}{dM} = -\delta(M) - 2\rho\sigma \quad , \tag{113}$$

where $F_n = 0$ when $E_n$ does. Hence the time of escape following capture may still be determined from the tabulated definite integral $I_p(M)$ defined in Eq. (98). The core-mantle coupling has the effect of modifying only the constant part of $\delta(M)$. If the times of entry into and escape from the separatrix are $M_0$ and $M_1$, respectively, then the value of $\dot{\zeta}$ at time $M_1$ according to (112) is just

$$\dot{\zeta}(M_1) = \dot{\zeta}(M_0)\ [P_k(e_0)/P_k(e_1)]^{1/2}\cdot\exp[\sigma(M_0-M_1)] \tag{114}$$

where $e_0$, $e_1$ denote the eccentricities at times $M_0$, $M_1$, respectively. With Formula (114) no numerical integration of either of equations (112) is needed.

## V. DISCUSSION OF RESULTS

Using the methods described in the preceding sections, we have computed capture probabilities for several (k = 3,4,5) spin-orbit resonances of Mercury, assuming originally rapid prograde rotation. The computations were repeated for each of the three tidal-torque models discussed in Section II for the following parameter values: the tidal parameter, $\alpha$, was increased by factors of 2 from $0.5 \times 10^{-9}$ to $1.6 \times 10^{-8}$, corresponding to values of Q from 400 to 12.5 respectively; the equatorial asymmetry parameter $\beta \equiv (3/2)(B-A)/C$ was increased by factors of 10 from $1.5 \times 10^{-6}$ to $1.5 \times 10^{-4}$; for the core-mantle moment-of-inertia ratio $\rho$ values of $10^{-2}$, $10^{-1}$, and 1.0 were used in addition to 0, or no distinct core at all; finally the core-mantle relative velocity damping constant $\sigma$ was increased by factors of $\sqrt{10}$ from $10^{-8}$ to $10^{-4}$, corresponding to exponential relaxation times of about $4 \times 10^{6}$ yr to 400 yr, respectively. These parameter ranges were chosen both on physical grounds and because early calculations showed these ranges to include the region of nontrivial results, i.e. nonzero and nonunity capture probabilities. We shall mention the most important general features of our numerical results, before describing them in detail:

(1) We found little difference between results obtained with different tidal torque models. With constant tidal lag angle (constant Q), with lag angle proportional to the angular rate of the tidal bulge, or with lag angle proportional to tidal amplitude, the results are remarkably similar.

(2) Without core-mantle coupling the probability of capture is inappreciable at resonances higher than k = 3 (spin period = 59 days), and remarkably <u>small</u> even at the k=3 resonance. Without core-mantle coupling this k = 3 probability depends only weakly on the tidal model and on the tidal parameter $\alpha$, but varies as the square root of the asymmetry parameter $\beta$. With $\beta = 1.5 \times 10^{-4}$ the greatest probability of

capture at k = 3 - about 0.1 - was obtained for the amplitude-proportional tidal lag with the rather extreme value $\alpha = 1.6 \times 10^{-8}$, which corresponds to an average Q less than 10. In view of the apparent capture of Mercury's spin into the k = 3 resonance, one is naturally curious whether core-mantle coupling could increase significantly the k = 3 capture probability.

(3) Core-mantle coupling does in fact act very strongly to increase the local capture probability at each resonance. By the local capture probability we mean the capture probability at the $k^{th}$ resonance given that no capture occurs at the higher (k+1, k+2,...) resonances. Since capture at any higher (k+1, k+2,...) resonance precludes capture at the $k^{th}$ resonance, it is evident that core-mantle coupling might actually reduce the net capture probability at the k = 3 resonance, rather than increase it. We find in fact that such a reduction occurs for a large range of values of $\sigma$. But there does exist a value $\sigma > 0$ which maximizes the net k = 3 capture probability for any given values of $\alpha$, $\beta$, and $\rho \neq 0$. The greatest net capture probability found is about 0.5.

(4) We find in general that the capture probability for given $\alpha$, $\beta$, and k, is essentially unchanged within the ranges investigated if both $\rho$ is decreased and $\sigma$ is increased by the same factor. This simplification might not have been expected, because the range of core-mantle relaxation times ($\approx \sigma^{-1}$) involved went from much shorter to a few times longer than the characteristic time of orbital eccentricity variation. Because of this $\rho\sigma$-product dependence, we use the intermediate value $\rho = 0.1$ throughout in the detailed presentation of results; probabilities for $\rho = 10^{-2}$ and $\rho = 1$ may be obtained by, e.g., reading the graphs using a value of $\sigma$ reduced or increased by a factor of 10. Capture probabilities for a "rigid" planet (i.e., a planet without a separately rotating core) are obtained as the limiting values as $\sigma$ approaches 0; for practical purposes the limit is reached with $\sigma = 10^{-9}$ (corresponding to a relaxation time of $4 \times 10^{7}$ yr).

The results of our computations for the local capture probability at the k = 3 resonance are summarized in Figs. 5, 6 and 7. In each

figure the local capture probability is shown (with a linear scale) as a function of $\sigma$(on a logarithmic scale), for several values of $\alpha$ and $\beta$, with $\rho = 0.1$. The three figures correspond to the three different tidal torque models: constant lag angle (Fig. 5), lag angle proportional to rate (Fig. 6), and proportional to amplitude (Fig. 7). In each figure we observe that as $\sigma \to 0$ the probability approaches a small constant value asymptotically, in the range 0.03 to 0.12. Although it cannot be seen on the scale of these figures, in each case (i.e. for any given $\alpha$ and tidal model) the asymptotic value of the probability varies as the square root of the asymmetry parameter $\beta$. This $\beta^{1/2}$ dependence also characterized the capture probability, when small, derived analytically for the case of fixed orbital eccentricity. A physical explanation of this latter functional behavior may be found in the interpretation of the capture probability as that fraction of the initial ensemble of systems which flows into the separatrix region (Section II). Since the density of systems (where nonvanishing) increases uniformly both near and in this region, the number of systems inside the separatrix region will increase at a rate proportional to its area. This area is in turn proportional to the square root of $\beta$ (Fig. 4).

In each figure the capture probability is seen to increase as $\sigma$ increases, and in most cases when the probability exceeds about 0.2 a fair approximation to the actual curve may be obtained in the form $P_c = A\sigma^B$ where the positive constants A and B vary from one curve to the next with B remaining in the range 0.6 to 1.0. If the appropriate power-law approximation of this form is found for each probability curve (i.e. corresponding to each tidal model and value of $\alpha$ and $\beta$), one discovers that the exponent B does not depend on the parameter $\beta$, but that the coefficient A in each approximation varies as $\beta^{B/2}$. This means that capture probability curves similar to those shown in Figs. 5, 6, and 7 for $\beta = 1.5 \times 10^{-4}$ but for smaller values of $\beta$, may be obtained by simply shifting the existing curves to the right along the $\sigma$-axis by one decade (power of 10) for every two decades(powers of 10) $\beta$ is reduced. In other words, the capture probability is a function

of $(\beta^{1/2}\sigma)$ for moderate-to-large probabilities. We recall that the asymptotic value of the capture probability (for $\sigma$ approaching 0) also varied as $\beta^{1/2}$.

These approximate and empirically-determined characteristics of the capture probability curves that we have obtained are mentioned because of the economy they allow in the presentation of an enormous amount of numerical data. Clearly the $\beta^{1/2}$ dependence of both large and small capture probabilities has its origin in Eq. (34), which arose in the analytical derivation of capture probabilities for the highly artificial fixed-eccentricity case. It would have been unjustified to claim that the $\beta^{1/2}$ dependence must necessarily follow also for the varying eccentricity case; however the fact that it does serves conceptually to organize our numerical results.

The local capture probabilities calculated for the k = 4 (44-day rotation period) resonance need not be discussed so extensively, because a simple formula describes each of the probabilities calculated with an absolute error less than 0.05. In general for the k = 4 resonance we find the local capture probability $P_c\{k=4\}$ given by

$$P_c\{k=4\} \approx C\alpha^{-1}\beta^{1/2}\rho\sigma \tag{115}$$

in which C = 7.5 for constant tidal lag; C = 9.5 for lag proportional to rate; and C = 5.9 for lag proportional to amplitude.

Formula (115) also describes the local capture probabilities calculated for the k = 5 (35-day rotation period) resonance with an absolute error generally less than 0.05. The empirically determined values of the constant C are, for the k = 5 resonance, C = 0.36 for constant tidal lag; C = 0.29 for lag proportional to rate; and C = 0.31 for lag proportional to amplitude.

In general we expect that for given $\alpha$, $\beta$, $\rho$, $\sigma$, and tidal model, the local capture probability will become smaller and smaller as we go to higher and higher resonance numbers $\underline{k}$, because the eccentricity

functions $P_k(e)$ grow smaller for reasonable orbital eccentricities. In the series representation of $P_k(e)$ we notice that the lowest power of $e$ with a nonzero coefficient is $k - 2$ for $k \geq 2$. Thus the $k = 5$ probabilities are substantially smaller than the $k = 4$ probabilities, which are in turn smaller than the $k = 3$ probabilities. In order to calculate the net probability of capture at the $k = 3$ resonance, therefore, we are probably justified in neglecting the $k = 6,7,8...$local capture probabilities, and using only the $k = 3,4$ and 5 local probabilities. If these local probabilities are represented by $p_3$, $p_4$, and $p_5$, then the net capture probability at the $k = 3$ resonance is approximately equal to $p_3 \cdot (1-p_4)(1-p_5)$. Combining the computed local probabilities in this manner we obtain the net probability curves shown in Figure 8. In the Figure we have plotted the net k=3 probability as a function of $\sigma$ for each of the three tidal torque models, for $\alpha = 0.4 \times 10^{-8}$, $\beta = 1.5 \times 10^{-4}$, and $\rho = 0.1$. Similar curves could be drawn for different values of these parameters, but the principal effect of varying $\beta$ and $\rho$ would be only to shift the curves to the right or left, as discussed earlier, and also to vary the small asymptotic (small-$\sigma$) probability with the square root of $\beta$. By inspection of formula (104) and Figures 5,6, and 7, evidently the principal effect of varying the tidal parameter $\alpha$ would also be a right-left shift, although some change in peak height, and in the case of amplitude-proportional lag with $\alpha = 1.6 \times 10^{-8}$ some broading of the peak toward the left, will also occur. The curves in Figure 8 are representative, however. The net probability goes abruptly to zero when $\sigma$ exceeds a certain value, because at this value capture at a higher ($k \geq 4$) resonance has become certain and $k = 3$ may not be reached. For sufficiently small values of $\sigma$ the local capture probabilities at the higher resonances become negligible while a residual (no-core) probability remains at $k = 3$. Between these extremes a peak value of the net probability is reached; for the set of parameters used in Figure 8 the peak is at $\sigma \approx 10^{-6}$, corresponding to a core-mantle velocity relaxation time of about 40,000 years.

## VI. CONCLUSION AND SUGGESTIONS FOR FUTURE STUDY

The two-dimensional mathematical model hitherto used to describe the evolution of Mercury's spin may be seriously in error. In the previous section we have shown that the present oscillations in orbital eccentricity, if typical for geologic time periods, imply that the probability of Mercury's having evolved to the 3:2 spin-orbit resonance is on the order of 0.02. This probability is too low to be believable. Therefore we have explored the possibility that Mercury has a liquid core dissipatively coupled to its mantle. This mechanism we have found to be probably incapable of significantly raising the 3:2 resonance capture probability. Core-mantle coupling does in fact act very strongly to increase the local capture probability at each resonance, i.e. the conditional probability of capture at the $k^{th}$ resonance given that no capture occurs at the higher (k+1, k+2,...) resonances. However, since capture at any higher resonance precludes capture at the $k^{th}$ resonance, it follows that core-mantle coupling might actually reduce the net capture probability at the $k^{th}$ resonance. We have found that such a reduction does occur for a large range of core-mantle coupling constants. But there exists a value of the coupling constant which maximizes the net k = 3 ($59^d$) capture probability for any given values of the tidal torque parameter, $\alpha$, the permanent equatorial asymmetry parameter, $\beta$, and core moment of inertia. The greatest net capture probability found is about 0.5, but the probability is less than 0.1 if the core-mantle coupling constant differs from the optimum value by more than a factor of 10. For a core whose moment of inertia is one-tenth that of the mantle, the 3:2 resonance capture probability is maximized when the core-mantle relaxation time is about 40,000 years.

The possibility that Mercury's average orbital eccentricity (now 0.175) was significantly higher ($\gtrsim$ 0.25) in the distant past could also lead to higher capture probability. Although given the current state of planetary orbit theory we have no reason to think that Mercury's average eccentricity was ever greater than it is now, at the same time neither can we prove with certainty that it was not. (Indeed

the whole question of the stability of the solar system remains theoretically unanswered.) How great must the average eccentricity be in order to raise the capture proability to one-half? We may obtain a quick and approximate answer to this question from the data summarized in Figure 9. In this Figure are plotted values of the net 3:2 resonance capture probability computed for various values of average eccentricity in the range 0.15 to 0.25, where for the purpose of illustration we have assumed three different manners of eccentricity variation about the mean value: In the first case (indicated by circular points in Figure 9) the time-varying eccentricity is assumed given by the expression

$$e(t) = e_0 + \sum_{k=1}^{2} e_k \sin[2\pi n_k (t/\tau_e) + \kappa_k] \tag{116}$$

where $e_0$ is the average eccentricity, $\tau_e = 5.52 \times 10^6$ years, $n_1 = 8$, $n_2 = 5$, $e_1 = -0.0255$, $e_2 = 0.0357$, $\kappa_1 = 194.7°$, $\kappa_2 = 152.63°$ [values obtained by truncating the harmonic expansion of Figure 3(b).]. In the second case (square points in Figure 9) we assume simply a sinusoidal oscillation of eccentricity with amplitude 0.04, given by

$$e(t) = e_0 + 0.04 \sin 2\pi t/\tau_e \quad ; \tau_e = 10^6 \text{ years}, \tag{117}$$

and in the third case (triangular points in Figure 9) we assume sinusoidal oscillation with twice the amplitude:

$$e(t) = e_0 + 0.08 \sin 2\pi t/\tau_e \quad ; \tau_e = 10^6 \text{ years}. \tag{118}$$

In these probability calculations no liquid core was included, and constant-lag-angle tidal friction was assumed with the parameter $\alpha = 0.4 \times 10^{-8}$ (cf. Section II.A); the equatorial asymmetry was $(B-A)/C = 10^{-4}$, corresponding to $\beta = 1.5 \times 10^{-4}$. The principal features of Figure 9 should be insensitive to the exact values used for $\alpha$ and $\beta$,

or to the choice of tidal model.

We find that no appreciable increase occurs in the 3:2 resonance capture probability until the average eccentricity is increased to very nearly 0.25. At this value the tidal torque averages separately to zero for the resonance spin rate, so that the capture probability approaches unity. If the average eccentricity were to exceed 0.25 (for this tidal model; slightly different values for other models), then the 3:2 resonance would never be reached, because tidal decay of Mercury's spin would cease at a somewhat faster spin rate. But if the spin rate decayed to tidal equilibrium while Mercury's average eccentricity exceeded 0.25, then a 3:2 resonance capture would be likely to result if the average eccentricity later decreased very slowly (say over $10^9$ years) to less than 0.25. We emphasize, however, that celestial mechanics (at present) suggest no mechanism which would produce such a secular change in orbital eccentricity. The subject of long-term (over $10^9$ years) changes in planetary orbits remains eminently open to further study.

Probably the most vulnerable assumption in our mathematical model of spin evolution is the planar assumption: that Mercury has always rotated about an axis nearly normal to the plane of its orbit. To reconsider this planar assumption must remain for future study. The three-dimensional equations are formidable, and their solution may be possible only by numerical integration. That such an effort may be worthwhile is indicated by the following observation: When a planet's spin angular velocity greatly exceeds its orbital mean motion and when the equator is inclined to the orbit plane, if due to friction the tidal distortion of the planet suffers an angular displacement ("lag") about the spin axis, then there will be a vector component of the tidal torque normal to the spin axis. The sense of this normal component is such that after integration over an orbital period the equatorial inclination, or angle between the spin angular velocity vector and the orbit pole, is increased. The magnitude of the normal component of the tidal torque vanishes as the inclination approaches either zero or 90 degrees, but

the magnitude is such that moderate inclinations (of a few degrees) are increased to large inclinations (exceeding 45 degrees) in about the same time as tidal friction reduces the spin magnitude to 10% of its original value.

An unpublished analysis by Peale (1968, private communication) indicates that although the effect of tidal friction on a rapidly rotating planet, as we have discussed, is to increase the tilt of the axis, on the other hand the effect of tidal friction on a slow, resonantly rotating planet is to reduce the tilt. If Peale's analysis is correct, we are led to the following picture of spin evolution for Mercury: Mercury's spin, like that of most of the other planets, was once rapid and direct, with a period between 10 and 20 hours, and an inclination of around 25 degrees. Through the effect of tidal friction the spin magnitude was reduced while the tilt increased until (possibly) a resonance rotation state was achieved with a severe axis tilt, perhaps nearly 90 degrees inclination. Then, while a spin-orbit resonance condition persisted, the spin axis was erected until the present configuration with small inclination was obtained. Whether a three-dimensional model might lead to significantly different capture probabilities than we have found for the two-dimensional model remains unanswered.

## CITED LITERATURE


Alsop, L.E., Sutton, G.H., and Ewing, M. 1961, J. Geophys. Res. 66, 2911.

Anderson, D.L., and Archambeau, C.B. 1964, J. Geophys. Res. 69, 2071.

Anderson, D.L., and Kovach, R.L. 1964, Proc. Natl. Acad. Sci. U.S. 51, 168.

Bellomo, E., Colombo, G., and Shapiro, I. 1966, paper presented before Symposium on Mantles of the Earth and Terrestrial Planets, March 1966.

_____ 1967, in Mantles of the Earth and Terrestrial Planets, ed. by S. K. Runcorn, (Interscience, New York).

Brouwer, D., and Clemence, G. 1961, in Planets and Satellites, G.P. Kuiper and B.M. Middlehurst, eds. (Univ. of Chicago Press, Chicago, 1961), p.31.

Brouwer, D., and van Woerkom, A.J.J. 1950, Astron. Papers Amer. Ephem. Naut. Almanac 13, Part 2, 83.

Camichel, H., and Dolfus, A. 1967, Compt. Rend. Paris B 264, 1765.

Cayley, A., 1859, Mem. Roy. Astron. Soc. 29, 191.

Cesari, L. 1963, Asymptotic Behavior and Stability Problems in Ordinary Differential Equations, 2nd ed., Academic, New York.

Chapman, C. 1967, Earth Planet. Sci. Lett. 3, 381.

Colombo, G. 1965, Nature 208, 575

_____ 1966, Astron. J. 71, 891.

Colombo, G., and Shapiro, I.I. 1965, Smithsonian Astrophys. Obs. Spec. Rept. 188R, 1.

Connes, J., Blum, P.A., Jobert, G.N., and Jobert, N. 1962, Ann. Geophys. 18, 260.

Counselman, C.C. 1968, A.I.A.A. J. 6, 1383.

Counselman, C.C., and Shapiro, I.I. 1969, In preparation.

Danby, J.M.A. 1962, Fundamentals of Celestial Mechanics, (MacMillan, New York) p. 98.

Darwin, G.H. 1908, "Tidal Friction and Cosmogeny," Scientific Papers (Cambridge University Press, New York), Vol. 2.

Dollfus, A. 1953, Bull. Soc. Astron. France 67, 61; Planets and Satellites G. P. Kuiper and B. M. Middlehurst, eds. (Univ. of Chicago Press, Chicago, 1961), p. 534.

Dyce, R.B., Pettengill, G.H., and Shapiro, I.I. 1967, Astron. J. 72, 351.

Floquet, G. 1883, Ecole Normale Superieure Annales 12, 47.

Goldreich, P., and Peale, S.J. 1966a, Nature 209, 1078.

Goldreich, P., and Peale, S.J. 1966b, Astron. J. 71, 425.

_____ 1967, Astron. J. 72, 662.

Goldreich, P., and Soter, S. 1966, Icarus 5, 375.

Gradshteyn, I.S., and Ryzhik, I.M. 1965, Table of Integrals, Series, and Products, 4th ed. (Academic Press, New York).

Gutenberg, B. 1959, Physics of the Earth's Interior (Academic Press, New York), Chapter 8.6.

Hagihara, Y. 1961, in Planets and Satellites, G. P. Kuiper and B. M. Middlehurst, eds. (Univ. of Chicago Press, Chicago, 1961), p. 95.

Jefferys, W.H. 1966, Science 152, 201.

Kelvin (Sir W. Thompson) 1863, Phil. Trans. Roy. Soc. 153.

_____ 1890, Math. and Phys. Papers, Vol. 3 (Cambridge), p. 351.

Kelvin and Tait, 1867, Nat. Philosophy, Part II (Oxford; 2nd ed. Cambridge 1879-1883).

Knopoff, L., and MacDonald, G.J.F. 1958, Revs. Modern Phys. 30, 1178.

_____ 1960, JGR 65, 2191.

Laslett, L. J., and Sessler, A.M. 1966, Science 151, 1384.

Liu, H.S., and O'Keefe, J.A. 1965, Science 150, 1717.

Love, A.E.H. 1892, Treatise on the Mathematical Theory of Elasticity (Cambridge Univ. Press, Cambridge), Vol. 1, pp.285-308.

McGovern, W.E., Gross, S.H., and Rasool, S.I. 1965, Nature 208, 375.

MacDonald, G.J.F. 1964, Rev. Geophys. 2, 467.

MacDonald, G.J.F., and Ness, N.F., 1961, J. Geophys. Res. 66, 1865.

Munk, W.H., and Macdonald, G.J.F., 1960, Rotation of the Earth, (Cambridge University Press, New York).

Nowroozi, A.A. 1968, J.G.R. 73, 1407.

Peale, S.J., and Gold, T. 1965, Nature 206, 1240.

Peselnick, L., and Outerbridge, W.F. 1961, J. Geophys. Res. 66, 581.

Pettengill, G.H., and Dyce, R.B. 1965, Nature 206, 1240.

Press, F., 1966, The Earth beneath the Continents, Geophys. Monograph 10, (American Geophysical Union, Washington, D.C.).

Schuler, M. 1923, Physik. Zeit. 24.

Smith, S. 1961; Ph.D. thesis, California Institute of Technology, Pasadena.

Sokolnikov, I.S. 1956, Mathematical Theory of Elasticity, 2nd ed., (McGraw-Hill, New York).

## Appendix A

## The Tidal Torque

### I. Tidal Friction

In the classical theory of tidal friction due to Darwin (1908), the tidal distortion of the planet's figure is assumed to be approximated by the equilibrium distortion of a homogeneous elastic sphere. To first order in (R/r), where r is the distance of the sun and R the surface radius of the planet, the tide-raising potential of the sun at the planet is given by a spherical harmonic function of second order. The equilibrium surface displacement ("tide") of a homogeneous elastic sphere subject to this potential is a surface harmonic of second order also, such that the height of the tide is simply proportional to the value of the disturbing potential everywhere on the surface. The effect of radial inhomogeneity in the body is only a change of scale of the tide; the form of the distortion is not changed. Small deviations from rotational symmetry in the body may be treated separately. Thus the elastic-sphere model may be a reasonable first approximation of a real planet if, for times characteristic of tidal motions, the planet behaves as a nearly-elastic solid, and provided that the natural periods of free oscillations are so short that resonance effects may be ignored. The effects of small deviations from perfect elasticity may be calculated by perturbation of this basic model.

At a point on the surface of a spherical planet of radius R where the zenith distance of the sun is $\xi$, the tide-raising potential of the sun is

$$W(\xi) = - (GM/r^3)R^2 \left( \frac{3}{2} \cos^2\xi - \frac{1}{2} \right) \qquad (A.1)$$

where G is the gravitational constant, M the solar mass, and r the sun-planet distance. Terms of higher order than the first in (R/r) are neglected. In the steady-state case (r and $\xi$ constant), the radial displacement, $\delta R$, of the surface of a spherically-symmetric planet is (Love, 1892)

$$\delta R(\xi) = -\frac{h}{g} W(\xi) \qquad (A.2)$$

where g is the surface gravitational field strength of the planet and h is a dimensionless constant known as the tidal Love number, which accounts for both the elastic and gravitational resistance to deformation of the sphere. For a homogeneous solid elastic sphere of mass density $\rho$ and modulus of rigidity $\mu$(Love, 1892),

$$h = \frac{5/2}{1+19\mu/2g\rho R} \quad . \qquad (A.3)$$

Eqs. (A.2) and (A.3) will be derived in the following section. Eq. (A.3) is often written in the form

$$h = \frac{5/2}{1+\mu_T} \qquad (A.4)$$

where the dimensionless parameter $\mu_T \equiv 19\mu/2g\rho R$ is known as the tidal effective rigidity. Elastic and gravitational restoring forces act in parallel to resist the tidal deformation, and $\mu_T$ expresses the ratio of elastic to gravitational effects. In the limit of zero elastic rigidity ($\mu_T \to 0$), the tidal Love number h approaches 2.5. For spheres of radially varying density the numerator in Eq.(A.4) may be replaced by a general parameter, $h_f$, known as the fluid Love number. A numerical value $h_f$ = 1.96 has been estimated for the Earth from tidal observations (Munk and MacDonald 1960, p.26); the 5/2 factor is adequate for our purposes, however.

Numerical estimates of the tidal effective rigidity and tidal Love number for Mercury can be made from values determined for the Earth. From seismic data, Gutenberg (1959, ch.8.6) has derived values for the modulus of a rigidity, $\mu$, of the Earth's mantle ranging from $0.7 \times 10^{12}$ dyne/cm$^2$ at a depth of 200 km to $2.8 \times 10^{12}$ dyne/cm$^2$ at 2800 km, and dropping off sharply at the outer core. Taking a value of $\mu = 10^{12}$ dyne/cm$^2$, g = 980 cm/sec$^2$, $\rho$ = 5.5 gram/cm$^3$, and $R = 6.4 \times 10^8$cm, for the Earth one calculates $\mu_T$ = 2.8. Observations of Earth tides, by

comparison, lead to a value of $\mu_T = 2.3$ (Munk and MacDonald, 1960, p.28), but this latter inference is somewhat complicated by the yielding of the oceans so that the fair agreement between these two values may be fortuitous. The modulus of rigidity value of $\mu = 10^{12}$ dyne/cm$^2$ leads to an estimated $\mu_T = 20$ for Mercury. (Note that $\mu_T \sim \mu/\rho^2 R^2$; the density of Mercury is about the same as the Earth's.)

The purely-elastic, steady-state model represented by Eq. (A.2) must be modified to include the effects of dissipation in the dynamic case. We first consider the effect of dissipation when the planet is rotating at a uniform rate, $\omega$, about an axis normal to the plane of a circular orbit around the sun. The constant orbital angular velocity, n, is measured in the same sense as $\omega$. As always in this paper, the dissipation is assumed to be so small that the equilibrium (dissipation-free) tidal distortion may be used to calculate the effect of the dissipation. In the limit of zero dissipation, of course, the equilibrium tide given by Eq. (A.2) is obtained, with the pattern of tidal distortion rotating to follow the sun at a rate $(n-\omega)$ with respect to the planet. (The attainment of this equilibrium configuration would require finite damping of the free oscillations of the elastic planet. The damping in this case may be taken arbitrarily small.) Viewed from a coordinate frame moving with the sun, the tidal distortion has exactly the form given by Eq. (A.2), independently of the value of $(n-\omega)$ in this lossless case. There is no tidal torque because of symmetry. This symmetry must be destroyed, however, if there is energy dissipation caused by the (sinusoidally) varying strain within the planet. Any energy dissipated must be supplied by means of a tidal torque opposing the planet's rotation with respect to the sun. If the mechanism of dissipation is presumed to be linear, i.e. "viscous", the modification of the tidal distortion is particularly simple (Munk and Macdonald, 1960, p. 22): the second harmonic form of the distortion is unchanged, but the entire pattern is rotated so that the axis of symmetry lags behind the apparent motion of the sun by an angle, $\delta$, which for small dissipation

is proportional to the relative rate, $(n-\omega)$, of solar motion. The lag thus corresponds to a small constant time delay of the tide. The height of the tidal bulge is unchanged to first order in $\delta$. The tidal torque, $\vec{T}$, due to the small tidal lag angle, $\delta$, may be calculated by the following procedure: the disturbance of the external gravitational potential of the planet caused by the surface displacement, $\delta R$, may be calculated by a straightforward application of potential theory by considering that an infinitesimally thin layer of surface mass density $\rho\delta R$ has been deposited on the spherical surface of the planet. As a function of radial distance, r, from the center of the planet, and of the angle, $\phi$, measured from the axis of symmetry of the tidal distortion, the potential, V, at an external point due to the surface layer is

$$V(r,\phi) = -\frac{3}{5} mR^2 \left(\frac{n^4 R}{g}\right) h\left(\frac{3}{2}\cos^2\phi - \frac{1}{2}\right) M^{-1} \qquad (A.5)$$

where $m = \frac{4}{3}\pi R^3 \rho$ is the mass of the planet. The tidal torque, $\vec{T}$, is obtained by differentiating (A.5) with respect to $\phi$, evaluating $\phi = \delta$, and multiplying by the solar mass, M, because the torque on the sun is equal and opposite to the sun's torque on the planet. If $C = \frac{2}{5} mR^2$ is substituted for the moment of inertia of the sphere the result may be written

$$\vec{T} = -\frac{9}{4} h\left(\frac{n^4 RC}{g}\right) \sin 2\delta \, \vec{k}, \qquad (A.6)$$

where $\vec{k}$ is a unit vector in the direction of the planet's angular velocity vector.

The linear, or "viscous" dissipation model which implies $\delta \sim (n-\omega)$ in Eq. (A.6) is very likely not a fair representation of the real mechanisms of tidal friction, which remain unknown even for the Earth. Studies of seismic attenuation in the Earth (Smith, 1961; Alsop et al., 1961; MacDonald and Ness, 1961; Connes et al., 1962; Anderson and Kovach, 1964; Anderson and Archambeau, 1964; Press, 1966; Nowroozi, 1968) and laboratory studies of acoustic attenuation in rocks (Knopoff and MacDonald, 1958; Peselnick and Outerbridge, 1961) both suggest, in fact, that the solid

dissipation mechanism is nonlinear, such that at least for strain amplitudes less than $10^{-8}$, the elastic "Q" is independent of amplitude and frequency for sinusoidal strain oscillations between $10^{-2}$ and $10^{6}$ Hz. The dimensionless parameter, Q, is defined as $2\pi$ times the ratio of the peak stored elastic energy, $E_{max}$, to the energy dissipated per cycle of the strain oscillation, $\Delta E$,

$$Q = \frac{2\pi E_{max}}{\Delta E} \tag{A.7}$$

$\Delta E$ is the difference between the mechanical work done to deform the material and the work returned by the relaxation of the deformation. In a linear system Q is inversely proportional to frequency for forcing frequencies much smaller than the natural frequency of free oscillations of the system and Q is equal to the ratio of the strain amplitude at resonance to the strain amplitude at low frequencies, for the same amplitude of applied stress. Non-linear dissipative mechanisms must be invoked (Knopoff and MacDonald, 1960) to account for the frequency independence of Q in certain solids.

What is the behavior of the tidal torque if the anelasticity of the planet is characterized by a constant elastic Q, independent of the amplitude or frequency of the sinusoidally varying tidal strain? The stored elastic strain energy, $E_{el}$, of the sphere, calculated for the equilibrium tidal distortion of Eq. (A.2), may be written in the form

$$E_{el} = \frac{9}{8} h \frac{\mu_T}{(\mu_T+1)} \left(\frac{n^4 RC}{g}\right) \tag{A.8}$$

In one cycle of tidal strain, corresponding to one half rotation of the planet with respect to the sun, the energy dissipated, $\Delta E$, must be

$$\Delta E = 2\pi Q^{-1} E_{el}. \tag{A.9}$$

This energy, $\Delta E$, is equal to the work done on the rotating planet by the tidal torque, $\vec{T}$. Eqs. (A.8) and (A.9) are compatible with (A.6) if the

tidal lag angle, $\delta$, is given by

$$\sin 2\delta = \left(\frac{\mu_T}{\mu_T+1}\right) Q^{-1} \quad . \tag{A.10}$$

The assumption of a constant tidal lag angle, $\delta$, independent of the rate, $(n-\omega)$, of relative tidal rotation might seem unreasonable because it implies a time lag of the tide which varies inversely with the rate $(n-\omega)$. This "variable memory", however, is an inherent feature of non-linear anelasticity models in which dissipative forces depending on relative displacement are assumed, e.g. hysteresis or Coulomb friction (Knopoff and MacDonald, 1960).

What value of Q is appropriate for the planet Mercury? Seismic studies of the Earth's mantle and laboratory measurements on granite suggest an upper bound on Q of a few hundred, due to simple solid anelasticity. For shear strains in the frequency range $3 \times 10^{-5}$ to $2 \times 10^{-4}$ Hz, values of Q reported for the Earth's mantle range from Q=100 for the upper 400 km, to Q=2000 for the lower mantle (refs. above). The effective average Q for the mantle appears to be between 200 and 400. Granite under laboratory conditions has a Q of several hundred in the frequency range 4 Hz to $10^7$ Hz (Peselnick and Outerbridge, 1961). Other solid dissipation mechanisms may also be important: e.g. MacDonald (1964) suggests that relative motions of large blocks of the Earth's crust in response to the tidal force account for about 40% of the total dissipation, which is characterized by a Q of about 30. Of course the motion of water on Earth provides a dissipation mechanism believed to be absent on Mercury.

It remains to consider the effect of orbital eccentricity on the tidal torque. When the orbital eccentricity is nonzero, the tidal potential (Eq. A.1) is time-varying: not only does the sun's distance vary, but the orbital angular velocity is variable according to Kepler's second law. In principle, however, the time-varying potential function can be expanded in an infinite sum of harmonic terms, each term having a constant amplitude, and a constant circular motion which is

a sum or difference of some multiple of the orbital mean motion, n, and the planet's (constant) spin angular velocity, $\omega$. (Cf. Appendix B.) The amplitudes of the component terms will be functions of orbital eccentricity, but for moderate values of the eccentricity the amplitudes will decrease rapidly with increasing angular arguments (higher multiples of the orbital mean motion.) Now if the planet is nearly elastic, the first approximation to the solution for the time varying tidal distortion (in which dissipation is ignored) is given by the sum of the individual distortions caused by the individual component terms in the Fourier-harmonic expansion of the potential, taken separately. From the previous discussion we recall that the response to each constant-amplitude, uniformly rotating potential term is a second-order surface spherical harmonic displacement, with height given by Eq. (A.2). Because the spin and orbital angular velocities of Mercury (corresponding to period of tens of days) are so much smaller than the natural frequencies of free oscillations of the elastic sphere (which correspond to periods of a few hours at most), the effects of resonance on the amplitude and phase of each component response may be neglected for all significant terms. As a result the composite tidal distortion (neglecting dissipation) is simply given by Eq. (A.2) with values of r and $\xi$ at every instant corresponding to the instantaneous position of the sun. The introduction of nonzero orbital eccentricity has no effect, therefore, on the dissipation-free tidal response. As in the circular-orbit case, there is no tidal torque when dissipation is absent.

The model of weak linear viscous dissipation remains easy to analyze. Assuming that all natural oscillation periods are very short compared to the tidal periods, then each harmonic component of the tide is delayed by the same constant time delay (i.e. by an angle proportional to the rotation rate of the component). When the components are added, therefore, the composite tide differs from the dissipation-free tide by only a constant time delay, or by an angle, $\delta$, which at any instant is approximately proportional to the instantaneous difference between the orbital angular velocity, $\dot{v}$, and spin rate, $\omega$. Following the previous derivation, the instantaneous tidal torque is found to be

$$\vec{T} = -\frac{9}{4} h \left(\frac{n^4 RC}{g}\right)\left(\frac{a}{r}\right)^6 \sin 2\delta \, \vec{k}, \qquad (A.11)$$

where a is the orbit semi-major axis, r is the instantaneous distance of the sun, and other terms have the same meanings as in Eq. (A.6).

When other, nonlinear dissipation models are considered, the calculation of the instantaneous tidal torque is in general more difficult than for the above, linear model. The basic perturbation method, of using the dissipation-free solution for the instantaneous tidal distortion in order to calculate the rate of energy dissipation by anelasticity, remains valid as long as the dissipation is "weak" ($Q >> 1$). Although the presence of stored elastic energy allows there to be a difference, instantaneously, between the rate of dissipation and the power supplied by the tidal torque, these two rates of energy transfer must balance over times long compared to the elastic relaxation time, defined as the quotient of the (typical or average) stored energy, divided by the (average) rate of dissiption. On an orbital time scale (days to hundreds of days), therefore, it is valid to consider the tidal torque at any time as given by Eq. (A.11), where the tidal lag angle, $\delta$, is determined in such a way as to balance the work done by the torque, and the rate of energy dissipation at each instant. The nonlinear, constant-Q dissipation model thus yields a constant lag angle, $\delta$, according to Eq. (A.10), where the sense of the tidal lag angle reverses if the sign of $(\dot{v}-\omega)$ reverses at some point in the orbit.

Because the significant actual mechanisms of tidal friction are unknown, even for the Earth, three different models of tidal friction are considered in this paper, corresponding to (1) $\delta$ = constant; (2) $\delta \sim (\dot{v}-\omega)$; and (3) $\delta \sim$ amplitude of the tide. The last model is intended to represent an amplitude-dependence of Q. These same three tidal models, referred to as "MacDonald's models," were considered by Goldreich and Peale (1966b) in their calculations of spin-orbit resonance capture probabilities for Mercury. These authors also con-

sidered a model ("Darwin's") in which the average (over an orbit) tidal torque suffers a finite step change as the planet's spin angular velocity passes from just above to below each resonance value, i.e. half-integer multiple of the orbital mean motion. This model, which incidentally leads to high capture probabilities, was justified by an erroneous argument: the tidal potential at the planet having been expanded in a Fourier time series (as we have discussed above), the $i^{th}$ Fourier component of the raised tide was considered to lag behind the $i^{th}$ potential component by a phase angle $\varepsilon_i$ which could be computed separately for each component from the value of the planet's "Q" corresponding to the frequency of the $i^{th}$ harmonic. In particular it was assumed that the phase lag $|\varepsilon_i|$ was the same for all components - this assumption admittedly having been suggested by the experimental evidence that the Q of rocks is independent of frequency. The contradiction inherent in this (so-called "Darwin's") tidal model should be evident from our discussion above. It is possible to compute separately the effect of each Fourier component of the tidal potential only when dissipation is absent (when the smallness of the strain assures the applicability of linear elasticity), or when the dissipation mechanism is itself linear. ("Linearity" here is equivalent to superposability of effects.) The assumption that the phase lags of harmonic strain components are independent of their frequencies is inconsistent with the assumption of linearity (superposability).

It should be noted that our own derivation of tidal torque models above depends on the assumption that the natural frequencies of free oscillations of the solid planet are very high compared to the planet's spin and orbital angular velocities. This assumption is probably justified for Mercury, but would certainly not be justified in a discussion of the tidal evolution of the Earth-Moon system.

## A.2 Tidal equilibrium of an elastic sphere

In this section we derive expressions (A.2) and (A.3) giving the equilibrium tidal distortion of an elastic sphere. For a homogeneous and isotropic incompressible elastic solid having shear modulus $\mu$ and mass

density $\rho$, equilibrium of elastic and gravitational forces requires that the components $u_i$ of the displacement along the Cartesian axes $x_i$ (i=1,2,3) satisfy (Sokolnikov, 1956, p.79):

$$\mu\nabla^2 u_i = \frac{\partial}{\partial x_i}(p+\rho U); \quad i = 1,2,3 \tag{A.12}$$

in which p is the hydrostatic pressure, U the gravitational potential, and $\nabla^2$ is the Laplacian operator:

$$\nabla^2 \equiv \sum_{i=1}^{3} \frac{\partial^2}{\partial x_i^2} \tag{A.13}$$

The condition of incompressibility is

$$\sum_{i=1}^{3} \frac{\partial u_i}{\partial x_i} = 0 \tag{A.14}$$

(This condition must apply to the interior of a planet to avoid gravitational collapse.) When the gravitational potential U is a known function Equations (A.12) and (A.14) provide four independent simultaneous partial differential equations for the four unknown functions $u_i$ (i=1,2,3) and p. When there is a tidal displacement of the surface of a self-gravitating body, however, then an additional component of the gravitational potential is due to the displaced mass at the surface.

In the absence of an externally originating tidal potential the gravitational potential distribution within a gravitating sphere is spherically symmetric and accompanied by a similar hydrostatic pressure distribution, such that the pressure everywhere balances the weight of the overlying mass. In an incompressible sphere these gravitational and hydrostatic forces are in equilibrium with zero elastic displacement. Because these spherically symmetric components of the potential and pressure fields contribute nothing to the displacement they will be ignored in the following discussion.

In order to compute the equilibrium tidal distortion of a self-gravitating elastic sphere we will consider first only the displacement produced directly by the externally applied tidal potential; then we will include the effects of the additional potential and surface pressure distributions due to the surface mass displacement.

The tide-raising potential, W, of the sun at a planet may be written in the form

$$W(x_1,x_2,x_3) = -n^2(x_3^2 - \frac{1}{2}x_1^2 - \frac{1}{2}x_2^2) \tag{A.15}$$

where n is the mean motion in a circular orbit (cf. Eq. A.1):

$$n^2 \equiv GM/a^3 = \text{constant} \tag{A.16}$$

and the Cartesian system of coordinates $x_i$ (i=1,2,3) has its origin at the center of mass of the planet, with the $x_3$-axis directed toward the sun. The general solution of Eqs. (A.12) for an elastic sphere was given by Kelvin (1863, 1890; Kelvin and Tait, 1867). For the special case U=W (Eq. A.15) the solution which satisfies the incompressibility condition (A.14) and yields zero surface tractions is

$$\begin{aligned} u_i &= \frac{\rho}{\mu}\left[\left(\frac{5}{38}r^2 - \frac{4}{19}R^2\right)\frac{\partial W}{\partial x_i} - \frac{2}{19}x_i W\right], \quad (i=1,2,3) \\ p &= \frac{2}{19}\rho W(x_1,x_2,x_3) \end{aligned} \tag{A.17}$$

where

$$r^2 \equiv \sum_{i=1}^{3} x_i^2 \tag{A.18}$$

and r = R defines the unstrained surface of the sphere. This solution (A.17) may be verified by direct substitution into Eqs. (A.12) and (A.14).

The displacement at the surface, obtained by evaluating (A.17) at r=R, is purely radial. The (positive-outward) displacement, $\delta R$, at a point on the surface may be written in the form

$$\delta R = - \frac{5\rho R}{19\mu} \left[W(x_1,x_2,x_3)\right]_{r=R} . \tag{A.19}$$

When the sphere is considered to be self-gravitating, there is an additional contribution to the internal gravitational potential due to the displaced mass at the surface, and a normal surface traction at r=R due to the weight of this thin surface layer. The internal (r<R) gravitational potential, V, generated by the surface displacement may be calculated simply if terms of order higher than the first in ($\delta R/R$) are neglected, by considering an equivalent surface mass layer of infinitesimal thickness and mass per area of $\rho\ \delta R$. If $\delta R$ is of the general form

$$\delta R = - (h/g)\left[W(x_1,x_2,x_3)\right]_{r=R} \tag{A.20}$$

where h is a constant and g is the surface gravity, then the surface-generated internal potential, V, is given by

$$V(x_1,x_2,x_3) = \frac{3}{5} hW(x_1,x_2,x_3), \quad (r<R) . \tag{A.21}$$

The normal surface traction at r=R due to the weight of the displaced mass is

$$-g\ \rho\delta R = \rho hW. \tag{A.22}$$

The displacements caused by this surface traction are completely equivalent to those caused by an applied potential of $U = -hW(x_1,x_2,x_3)$ with <u>no</u> traction. This fact becomes evident if the following particular solution to Eqs. (A.12) and (A.14) is considered:

$$u_i = 0, \ (i = 1,2,3)$$

$$p = \rho h W(x_1, x_2, x_3) \tag{A.23}$$

The net effect of the gravitating surface layer on the elastic displacements is thus obtained by adding

$$V' = -\frac{2}{5} hW \tag{A.24}$$

to the internal potential. The net surface displacement, $\delta R$, is then given by Eq. (A.20) with

$$h = \frac{5g\rho R}{19\mu} \left(1 - \frac{2}{5} h\right) \tag{A.25}$$

or

$$h = \frac{5/2}{1+19\mu/2g\rho R} \quad . \tag{A.3}$$

The stored elastic strain energy, $E_{el}$, associated with this deformation may be obtained by direct integration of the energy density

$$\frac{1}{4} \mu \sum_{i=1}^{3} \sum_{j=1}^{3} \left(\frac{\partial u_i}{\partial x_j} + \frac{\partial u_j}{\partial x_i}\right)^2 \tag{A.26}$$

over the sphere ($r<R$).

## Appendix B

## Expressions for the Average Dimensionless Tidal Torque

If the tide lags the sun by a constant lag angle, independent of the amplitude or rate of the tidal strain (model 1), the dimensionless tidal torque is $\alpha T$, where $\alpha$ is a small positive constant and T has the form (Eq. 4 of text)

$$T(e,\omega,M) = - \left(\frac{1+e \cos v}{1-e^2}\right)^6 \operatorname{sgn}\left(\omega - \frac{dv}{dM}\right) \tag{B.1}$$

in which e is the orbital eccentricity; $\omega$, the dimensionless planetary spin rate; M, orbital mean anomaly; and v, true anomaly. The average dimensionless tidal torque, $T_0$, is defined by

$$T_0(e,\omega) = \frac{1}{2\pi} \int_0^{2\pi} T_0(e,\omega,M)\,dM. \tag{B.2}$$

The binomial formula may be used to expand $(1+e \cos v)^6$. The difference $(\omega - dv/dM)$ changes sign only if

$$(1-e)^{1/2}/(1+e)^{3/2} < \omega < (1+e)^{1/2}/(1-e)^{3/2} \quad . \tag{B.3}$$

In this case break the integral in (B.2) into separate integrals for $0 \leq v \leq v_c$, $v_c \leq v \leq \pi$, etc., where

$$v_c = \cos^{-1}\left\{\frac{1}{e}\left[(1-e^2)^{3/4}\omega^{1/2}-1\right]\right\} ; \qquad 0 \leq v_c \leq \pi \quad . \tag{B.4}$$

The derivative, $T_0'$, of the average dimensionless tidal torque, defined by

$$T_0'(e,\omega) \equiv \frac{\partial}{\partial\omega} T_0(e,\omega) \tag{B.5}$$

is obtained most directly by differentiation of (B.2) before the integration is performed. We obtain in this manner, when

$$\omega \leq (1-e)^{1/2}/(1+e)^{3/2}:$$

$$T_0(e,\omega) = (1-e^2)^{-9/2}(1+3e^2 + \frac{3}{8} e^4) \; ; \; T_0'(e,\omega) = 0 \; ; \tag{B.6.1}$$

when

$$\omega \geq (1+e)^{1/2}/(1-e)^{3/2}:$$

$$T_0(e,\omega) = -(1-e^2)^{-9/2}(1+3e^2+ \frac{3}{8} e^4) \; ; \; T_0'(e,\omega) = 0 \; ; \tag{B.6.2}$$

otherwise (B.3):

$$\begin{aligned} T_0(e,\omega) = -(1-e^2)^{-9/2}(2\pi)^{-1} \{ & 2(\pi-2v_c) \\ & -16\, e \sin v_c \\ & + 6e^2(\pi-2v_c-2 \sin v_c \cos v_c) \\ & -(16/3)e^3(3 \sin v_c - \sin^3 v_c) \\ & +(1/8)\, e^4(6\pi-12v_c-12\sin v_c \cos v_c - 8 \sin v_c \cos^3 v_c)\} \end{aligned} \tag{B.6.3}$$

$$T_0'(e,\omega) = -\omega^{3/2}/[\pi e(1-e^2)^{3/4} \sin v_c]$$

in which $v_c$ has the definition (B.4).

When the tidal lag angle is proportional to rate (model 2), the form of the tidal function, T, becomes (Eq.9 of text)

$$T(e,\omega,M) = - \left( \frac{1+e \cos v}{1-e^2} \right)^6 (\omega - \frac{dv}{dM}). \tag{B.7}$$

In this case $T_0$, defined by (B.2), and $T_0'$, defined by (B.5), become respectively

$$T_0(e,\omega) = (1-e^2)^{-6}(1+\frac{15}{2}e^2+\frac{45}{8}e^4+\frac{5}{16}e^6)-(1-e^2)^{-9/2}(1+3e^2+\frac{3}{8}e^4)\cdot\omega$$

$$T_0'(e,\omega) = -(1-e^2)^{-9/2}(1+3e^2+\frac{3}{8}e^4). \qquad (B.8)$$

When the tidal lag angle is proportional to the strain amplitude (model 3), we have (Eq. 10 of text)

$$T(e,\omega,M) = -\left(\frac{1+e\cos v}{1-e^2}\right)^9 \operatorname{sgn}\left(\omega - \frac{dv}{dM}\right) . \qquad (B.9)$$

The method used above for model 1 yields when

$$\omega \leq (1-e)^{1/2}/(1+e)^{3/2} \quad :$$

$$T_0(e,\omega) = (1-e^2)^{-15/2}(1+\frac{21}{2}e^2+\frac{105}{8}e^4+\frac{35}{16}e^6)$$

$$T_0'(e,\omega) = 0 \; ; \qquad (B.10.1)$$

when

$$\omega \geq (1+e)^{1/2}/(1-e)^{3/2} \quad :$$

$$T_0(e,\omega) = -(1-e^2)^{-15/2}(1+\frac{21}{2}e^2+\frac{105}{8}e^4+\frac{35}{16}e^6) \qquad (B.10.2)$$

$$T_0'(e,\omega) = 0 \; ;$$

otherwise (B.3):

$$T_0(e,\omega) = \frac{1}{\pi}(1-e^2)^{-15/2}$$

$$\cdot \left\{ [1+\frac{21}{2}e^2+\frac{105}{8}e^4+\frac{35}{16}e^6]\ (2v_c-\pi) \right.$$

$$\left. +[14e+\frac{105}{2}e^3+\frac{105}{4}e^5+\frac{35}{32}e^7]\ \sin v_c \right.$$

$$+\left[\frac{21}{2}\,e^2+\frac{35}{2}\,e^4+\frac{105}{32}\,e^6\right]\sin 2v_c$$

$$+\left[\frac{35}{6}\,e^3+\frac{35}{8}\,e^5+\frac{7}{32}\,e^7\right]\sin 3v_c$$

$$+\left[\frac{35}{16}\,e^4+\frac{21}{32}\,e^6\right]\sin 4v_c \qquad \text{(B.10.3)}$$

$$+\left[\frac{21}{40}\,e^5+\frac{7}{160}\,e^7\right]\sin 5v_c$$

$$+\left[\frac{7}{96}\,e^6\right]\sin 6v_c$$

$$+\left[\frac{1}{224}\,e^7\right]\sin 7v_c \Big\}$$

$$T_0'(e,\omega) = -\omega^3/[\pi e \sin v_c(1-e^2)^{3/2}]$$

in which $v_c$ has the definition (B.4).

The result expressed in (B.6), for the average tidal torque in the case of constant lag (model 1), was first published by Colombo and Shapiro (1965). Goldreich and Peale (1966) have published expressions equivalent to (B.6), (B.8), and (B.10) for all three tidal models; unfortunately their expressions for models 2 and 3 contain several errors.

## Appendix C.
## Series Solution of the Spin Equation of Motion

The spin equation of motion (Eq. 11 of text) is written in the form

$$\frac{d\theta}{dM} = \omega$$

$$\frac{d\omega}{dM} = -\beta\left\{ \left[\frac{1+e\cos v}{1-e^2}\right]^3 \sin 2(\theta-v) \right.$$

$$\left. +\gamma\left[\frac{1+e\cos v}{1-e^2}\right]^6 \operatorname{sgn}\left[\frac{d\theta}{dM} - \frac{dv}{dM}\right] \right\} \quad . \tag{C.1}$$

A solution is sought as a power series in $\beta$:

$$\theta(M) = \sum_{i=0}^{\infty} \beta^i \theta_i(M)$$

$$\omega(M) = \sum_{i=0}^{\infty} \beta^i \omega_i(M) \tag{C.2}$$

Substituting these expansions into the equations of motion and equating separately the coefficients of terms multiplied by the same power of $\beta$, as described in Section II.C, we obtain the members $\theta_i(M)$, $\omega_i(M)$ of the power series solution (C.2):

$$\omega_0(M) = \omega_0' = \text{const}$$

$$\theta_0(M) = \theta_0' + \omega_0' M \tag{C.3}$$

$$\omega_1(M) = \sum_{j=-\infty}^{\infty} P_j(e) C_2(j) - \gamma\{T_0(e,\omega_0')M + \sum_{j=1}^{\infty} j^{-1} T_j(e,\omega_0') \sin j M \}$$

$$\theta_1(M) = \sum_{j=-\infty}^{\infty} \frac{P_j(e)}{(2\omega_0'-j)} \{s_2(j) - M \cos 2\theta_0'\} \qquad (C.4)$$

$$-\gamma \{\tfrac{1}{2} T_0(e,\omega_0')M^2 - \sum_{j=1}^{\infty} j^{-2} T_j(e,\omega_0')[\cos jM - 1]\}$$

$$\omega_2(M) = \sum_{j,k} \frac{P_j P_k}{(2\omega_0'-k)^2} \left\{C_4(j+k) + \frac{\cos(j-k)M-1}{(j-k)} + 2 \sin(2\theta_0')s_2(j)\right.$$

$$\left. + 2 \cos 2\theta_0' \left[\frac{(2\omega_0'-k)}{(2\omega_0'-j)}\right][C_2(k)+M \sin \eta(j)]\right\}$$

$$+ \gamma \sum_j \frac{P_j}{(2\omega_0'-j)} \left\{\frac{T_0}{(2\omega_0'-j)} [2M \cos \eta(j) - s_2(j) + M^2(2\omega_0'-j)\sin \eta(j)]\right.$$

$$\left. - T_0'[s_2(j) - M \cos 2\theta_0']\right\}$$

$$+ \gamma \sum_j P_j \left\{k^{-2} T_k [2s_2(j) - s_2(j-k) - s_2(j+k)]\right.$$

$$\left. - \frac{T_k'}{(2\omega_0'-j)} \left[s_2(k-j) + s_2(k+j) - \frac{\cos 2\theta_0' \sin jM}{j}\right]\right\}$$

$$+ \gamma^2 \left\{\frac{T_0 T_0'}{2} M^2 + \sum_k \left[T_0 T_k' \frac{\sin kM}{k} - T_0' T_k \frac{\cos kM - 1}{k^2}\right]\right.$$

$$\left. + \sum_{j,k} \frac{T_j' T_k}{2k} \left[\frac{\cos(j+k)M-1}{(j+k)}\right]\right\} \qquad (C.5)$$

$$\theta_2(M) = \sum_{j,k} \frac{P_j P_k}{(2\omega_0'-k)^2} \left\{\frac{s_4(j+k) - M \cos 4\theta_0'}{(4\omega_0'-j-k)} + \frac{\sin(j-k)M - (j-k)M}{(j-k)^2}\right.$$

$$\left. - 2 \sin 2\theta_0' \left[\frac{C_2(j)+M \sin 2\theta_0'}{2\omega_0'-j}\right]\right.$$

$$+ 2 \cos 2\theta_0' \left[ \frac{2s_2(k) - M(\cos 2\theta_0' + \cos\eta(k))}{2\omega_0' - j} \right] \Bigg\}$$

$$+ \gamma \sum_j \frac{T_0}{(2\omega_0' - j)^2} \left[ 6C_2(j) + 4M \sin \eta(j) - (2\omega_0' - j)M^2 \cos \eta(j) + 2M \sin 2\theta_0' \right]$$

$$+ T_0' \left[ C_2(j) + M \sin 2\theta_0' + \frac{1}{2} (2\omega_0' - j)M^2 \cos 2\theta_0' \right]$$

$$+ \gamma \sum_{j,k} P_j \Bigg\{ k^{-2} T_k \left[ \frac{C_2(j-k) + M \sin 2\theta_0'}{(2\omega_0' - j + k)} + \frac{C_2(j+k) + M \sin 2\theta_0'}{(2\omega_0' - j - k)} \right.$$

$$\left. - 2 \frac{C_2(j) + M \sin 2\theta_0'}{(2\omega_0' - j)} \right] + \frac{T_k'}{(2\omega_0' - j)} \left[ \frac{C_2(j-k) + M \sin 2\theta_0'}{2(2\omega_0' - j + k)} \right.$$

$$\left. + \frac{C_2(j+k) + M \sin 2\theta_0'}{2(2\omega_0' - j - k)} + \cos 2\theta_0' \left( \frac{1 - \cos j M}{j} \right) \right] \Bigg\}$$

$$+ \gamma^2 \Bigg\{ T_0\, 0' \frac{M^3}{6} + \sum_k \left[ T_0 T_k' \left( \frac{1 - \cos kM}{k^2} \right) - T_0' T_k \left( \frac{\sin kM - kM}{k^3} \right) \right]$$

$$+ \sum_{j,k} \frac{T_j' T_k}{2k} \left[ \frac{\sin(j+k)M - (j+k)M}{(j+k)} + \frac{\sin(k-j)M - (k-j)M}{(k-j)^2} \right] \Bigg\} , \qquad \text{(C.6)}$$

where

$$S_n(j) \equiv \frac{\sin[n\theta_0' + (n\omega_0' - j)M] - \sin n\theta_0'}{(n\omega_0' - j)} \qquad , \qquad \text{(C.7)}$$

$$C_n(j) \equiv \frac{\cos[n\theta_0' + (n\omega_0' - j)M] - \cos n\theta_0'}{(n\omega_0' - j)}$$

$$\eta(j) \equiv 2\theta_0' + (2\omega_0' - j)M \qquad \text{(C.8)}$$

and the coefficients $P_j$, $T_j$, $T_j'$ are given by Counselman and Shapiro, 1969.

For the special case e = 0 we find

$$\omega_3(M)\Big|_{e=0} = (2\omega_0'-2)^{-4}\cdot\{\ (3+4\cos 4\theta_0')C_2(2)$$

$$+\ (\frac{9}{2}\sin 4\theta_0')S_2(2)$$

$$+\ (6\cos 2\theta_0')C_4(4) + (4\sin 2\theta_0')S_4(4)$$

$$+\ (6+3\cos 4\theta_0')M\sin\eta(2)$$

$$-\ (2\sin 4\theta_0')\ M\cos\eta(2)$$

$$+\ (2\cos 2\theta_0')\ M\sin 2\eta(2)$$

$$-\ (1+\cos 4\theta_0')(2\omega_0'-2)M^2\cos\eta(2)$$

$$+\ (2\omega_0'-2)^{-1}[\ \cos^3\eta(2)-\cos^3 2\theta_0']\} \qquad (C.9)$$

$$\theta_3(M)\Big|_{e=0} = (2\omega_0'-2)^{-5}\cdot\{(12+9\cos 4\theta_0')S_2(2)-\frac{13}{2}\sin 4\theta_0'C_2(2)$$

$$+\ 4\cos 2\theta_0'\ S_4(4)-2\sin 2\theta_0'C_4(4)-(2\sin 4\theta_0')M\sin\eta(2)$$

$$-(8+6\cos 4\theta_0')M\cos\eta(2) - (\cos 2\theta_0')M\cos 2\eta(2)$$

$$-(2+2\cos 4\theta_0')M^2\sin\eta(2) - (\frac{9}{2}\sin 4\theta_0')M\sin 2\theta_0'$$

$$-(3+4\cos 4\theta_0')M\cos 2\theta_0' - (2\sin 2\theta_0')M\sin 4\theta_0'$$

$$-(3\cos 2\theta_0')M\cos 4\theta_0'$$

$$-\ \frac{\sin^3\eta(2)-\sin^3 2\theta_0'}{6(\omega_0'-1)}\ - M\cos^3 2\theta_0'\ \} \qquad (C.10)$$

TABLE 1

Constants in the solution for the secular variations of Mercury's orbital eccentricity, from Brouwer and van Woerkom (1950).

| k | $N_{1k}$ | $\phi_k$ (degrees) | $s_k$ (arcsec/ Julian year) |
|---|---|---|---|
| 1 | +.1745 | 92.18 | - 5.46 |
| 2 | -.0255 | 196.88 | - 7.34 |
| 3 | +.0015 | 335.22 | -17.33 |
| 4 | -.0017 | 317.95 | -18.00 |
| 5 | +.0357 | 29.55 | - 4.30 |
| 6 | +.0010 | 125.12 | -27.77 |
| 7 | +.0004 | 131.94 | - 2.72 |
| 8 | .0000 | 69.02 | - 0.63 |
| 9 | -.0002 | 293.98 | +19.17 |
| 10 | +.0001 | 220.69 | -51.24 |

## Figure Captions

Figure 1. Spin-orbit geometry: $\underline{v}$ is the orbital true anomaly; $\theta$ is the angle of rotation about the spin axis (normal to the orbital plane), measured between the orbit major axis and the planet's equatorial axis of minimum moment of inertia; $\underline{r}$ is the distance between the centers of mass of Sun and Mercury.

Figure 2(a). Phase plane geometry of resonance capture: $\theta$ (modulo $\pi$) is the instantaneous angle of rotation observed stroboscopically at perihelion passage; $\dot{\theta}$ is the rotation rate relative to the resonance rotation rate. (Thus the $\theta$-axis corresponds to the resonance rate.) C and D denote the unstable and stable equilibrium or fixed points, respectively. Continuous curves represent sequences of points $(\theta,\dot{\theta})$ at successive perihelia which converge asymptotically to C. Points A and B lying on these curves have the same abscissa as C. The curves shown were actually computed and plotted from Eq.(23) using exaggerated parameter values ($\theta_{eq} \simeq \alpha T_0/2\beta P_k = -0.1$) in order to display better the behavior near A, B, and C. With realistic parameter values ($\alpha << \beta$) the points A, B, and C would appear on the scale of this Figure to coincide at $(0,-\pi/2)$. The capture probability for the case drawn is 0.5.

Figure 2(b). Phase plane geometry for escape from resonance [refer to Fig. 2(a)]: Both A and D are unstable equilibria. Phase point sequences shown originating near A have the same value of abscissa as A at points B and C. Sequences (not shown) spiralling outward from D must cross line segment $\overline{AB}$ or $\overline{AC}$ (escape to faster or slower spin, respectively). For the case drawn here $\theta_{eq} = -0.05$, and the probabilities of escape to faster and slower spin are 1/4 and 3/4, respectively.

Figure 3(a) and (b). Variation of Mercury's orbital eccentricity with time for 25 million years from 1950: (a) according to Brouwer and van Woerkom (1950); (b) a periodic function with $\tau = 5.52 \times 10^6$ yr (see text).

Figure 4. Contours in the phase $(\theta,\dot{\theta})$ plane of the normalized energy function $E_n$ used to trace spin evolution.

Figure 5. Local capture probability at the k=3 (59 day rotation period) resonance as a function of the core-mantle coupling constant, $\sigma$, for various fixed values of the tidal friction parameter, $\alpha$, and the equatorial asymmetry, $\beta$, with core-mantle moment-of-inertia ratio $\rho$=0.1 and constant tidal lag angle. The orbital eccentricity variation of Figure 3(b) was assumed.

Figure 6. Same as Figure 5, except that the tidal lag angle is assumed proportional to the tidal rotation rate.

Figure 7. Same as Figure 5, except that the tidal lag angle is proportional to the height of the tide.

Figure 8. Net capture probability for the k=3 (59 day rotation period) resonance as a function of the core-mantle coupling constant, $\sigma$, for typical values of tidal friction, equatorial asymmetry, and core size parameters, and three different tidal friction models. Cutoff for large $\sigma$ is due to prior capture at higher (k=4,5,...) resonance. Core-mantle relaxation time $\sim 1/\sigma$; $\sigma = 10^{-6}$ corresponds to about 40,000 years.

Figure 9. Effect upon local (k=3) resonance capture probability of changing average value of orbital eccentricity. Circular points were computed and plotted for the eccentricity variation of Figure 3(b), but with the different average values shown here. Square and triangular points correspond to simple sinusoidal variation of eccentricity with period $10^6$ yr and amplitudes 0.04 and 0.08, respectively. Computed for constant tidal lag angle and no core-mantle coupling.

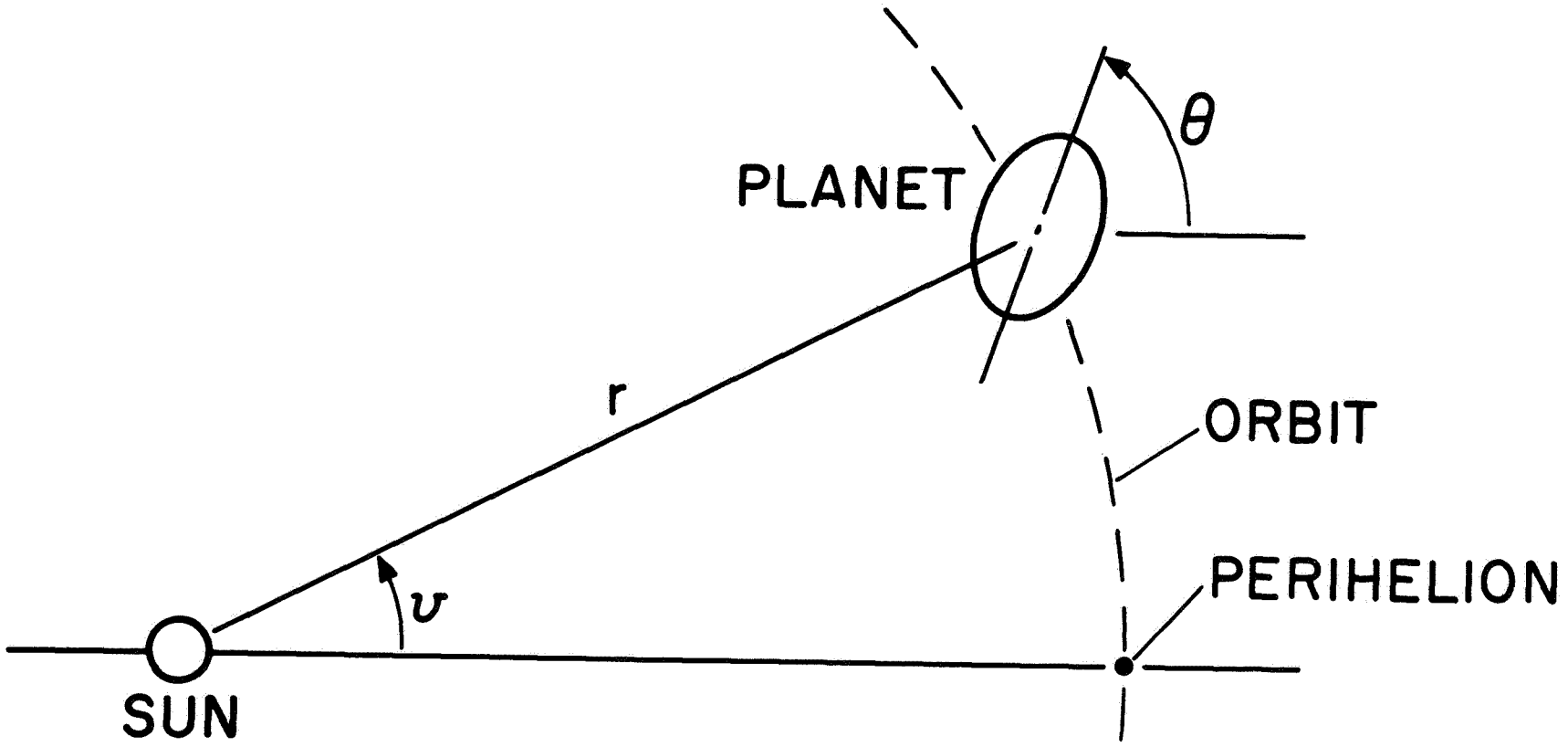


Thesis Figure 1

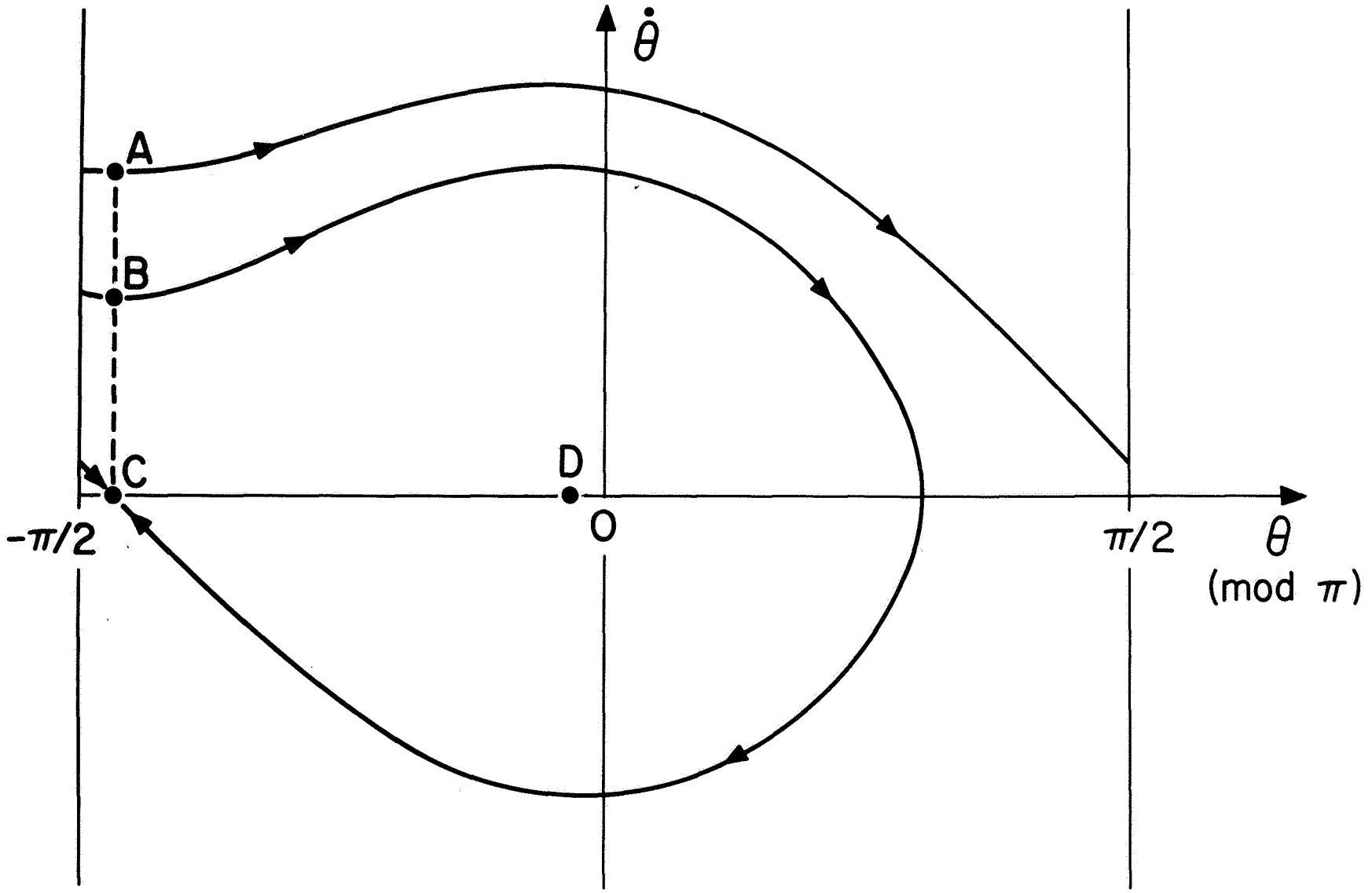


Thesis Figure 2(a)

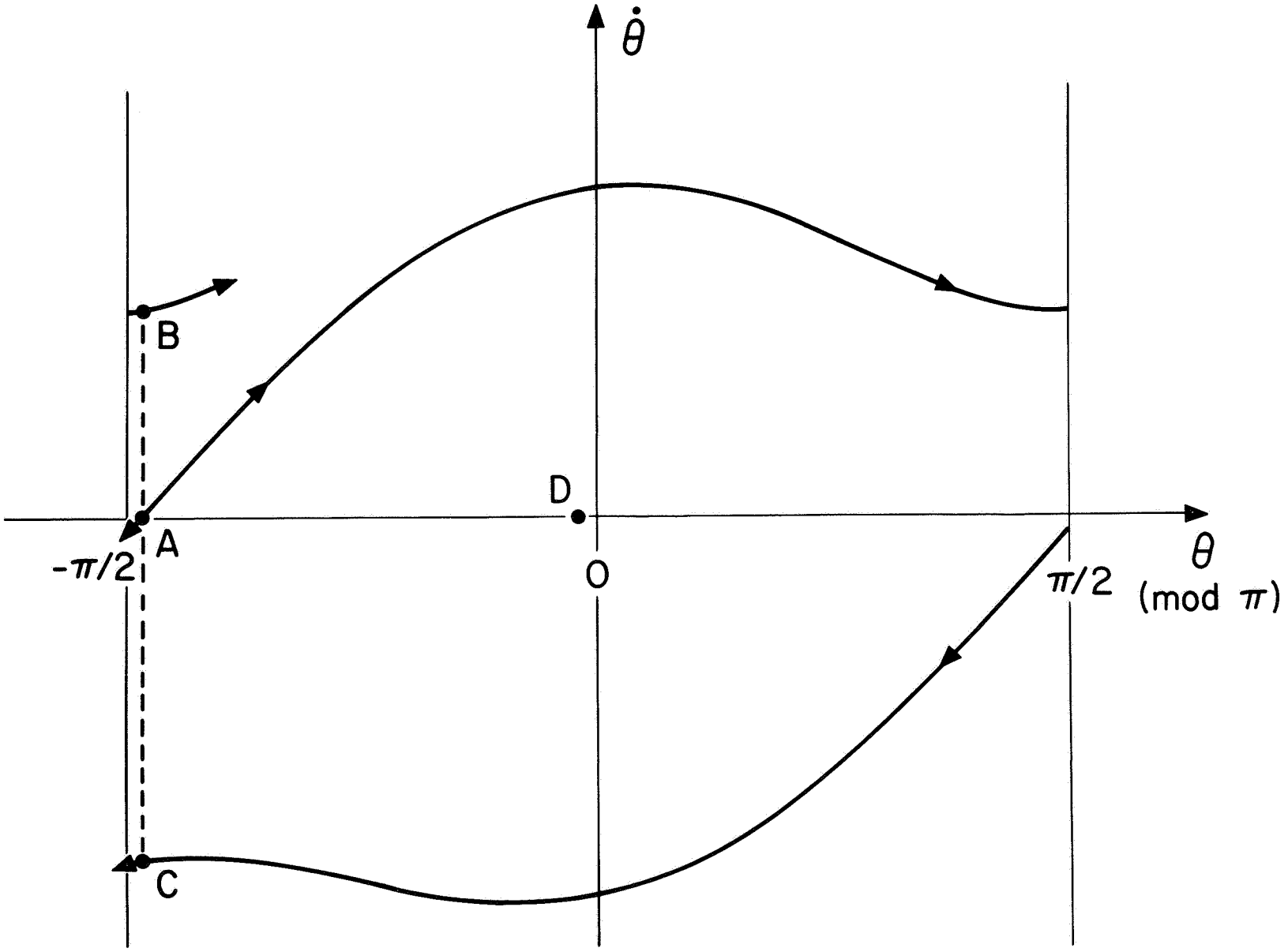


Thesis Figure 2(b)

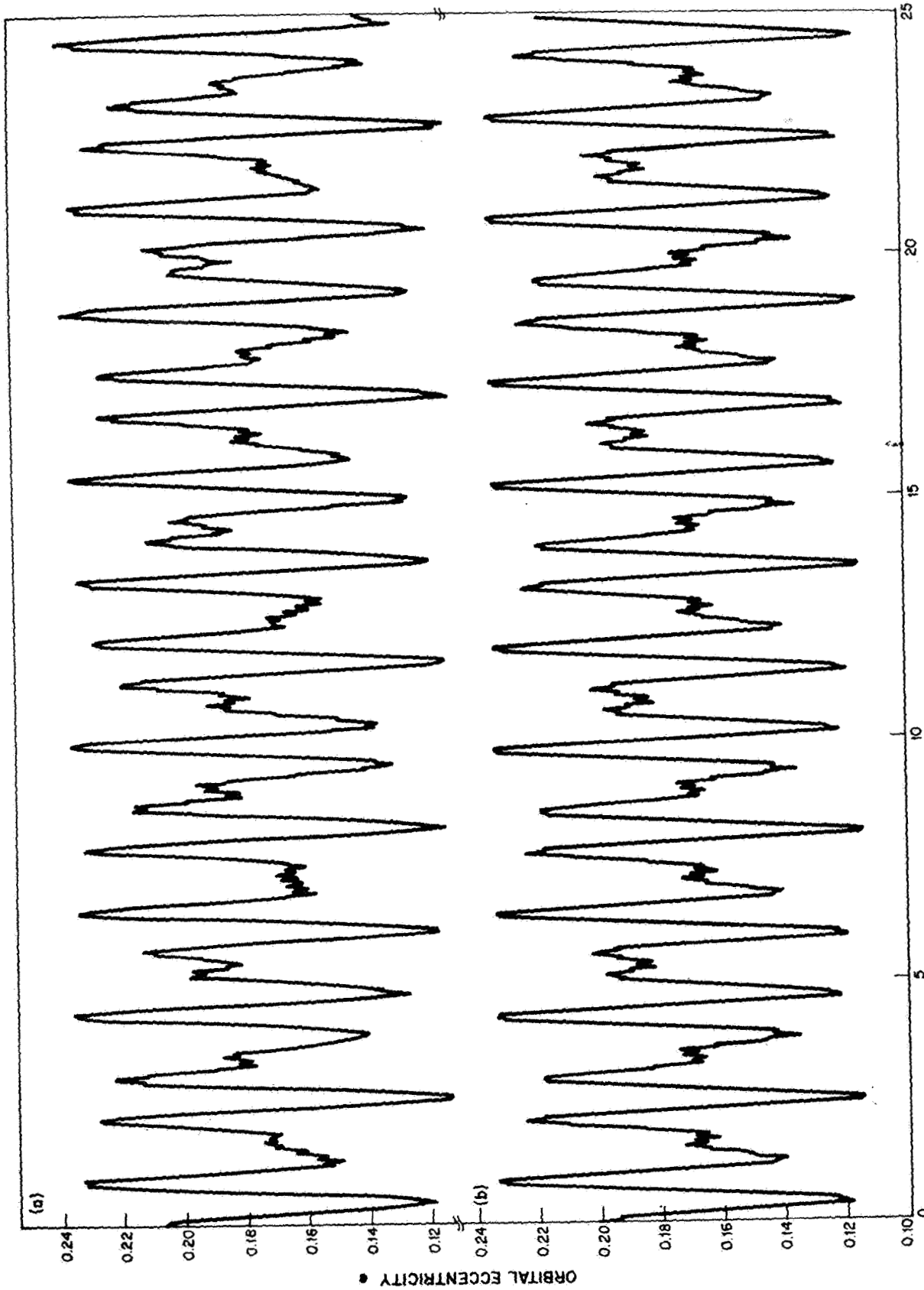


Thesis Figure 3, (a) and (b)

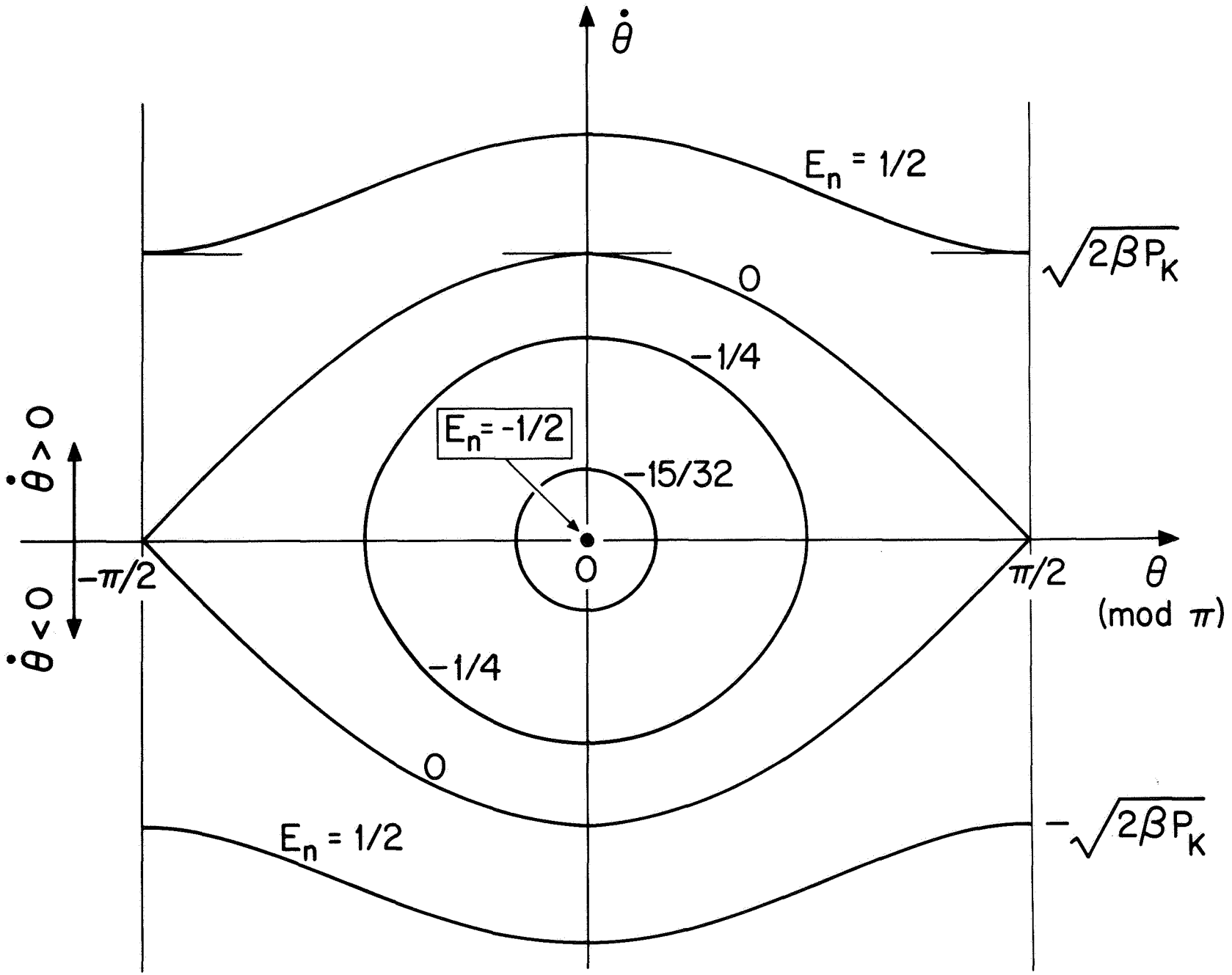


Thesis Figure 4

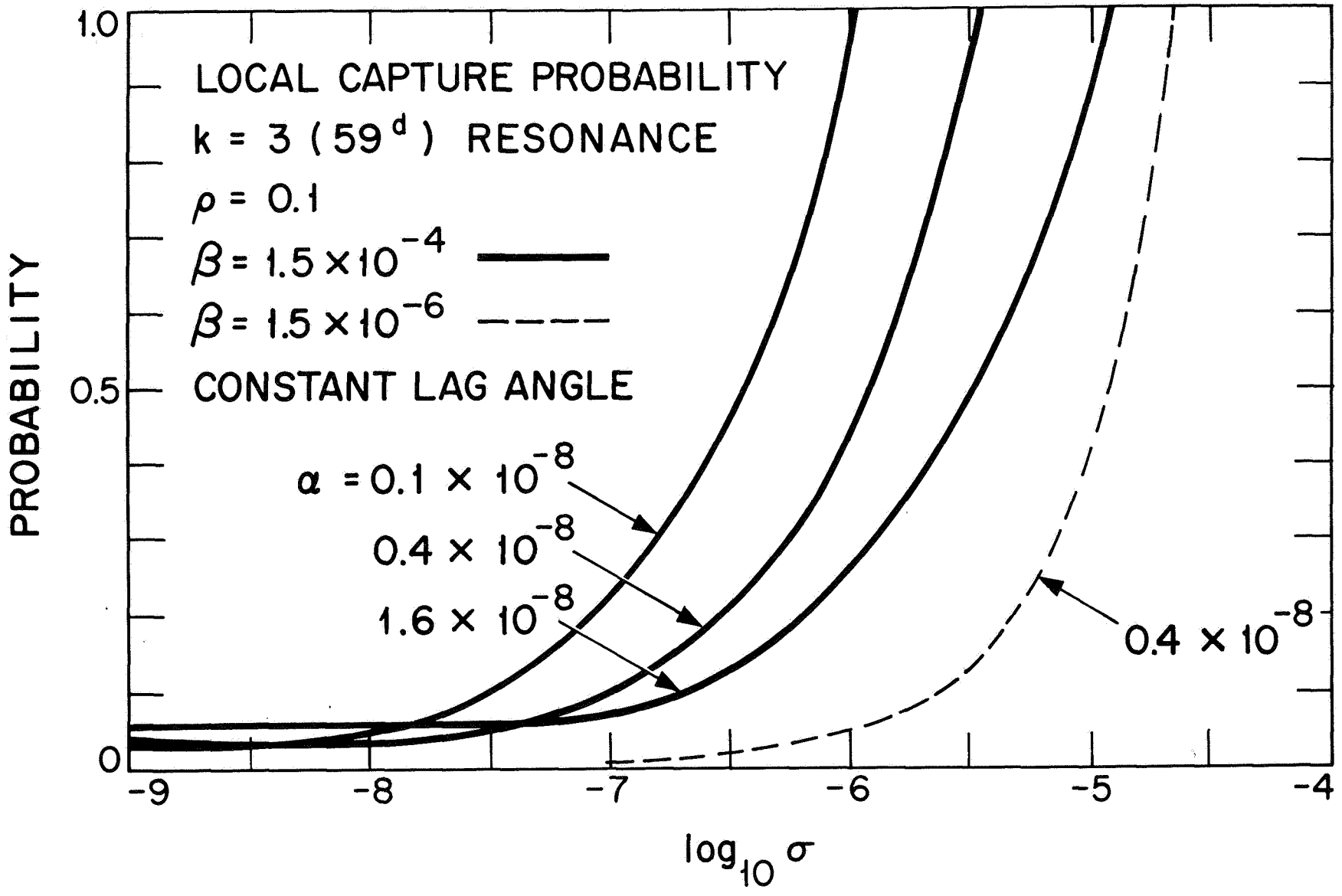


Thesis Figure 5

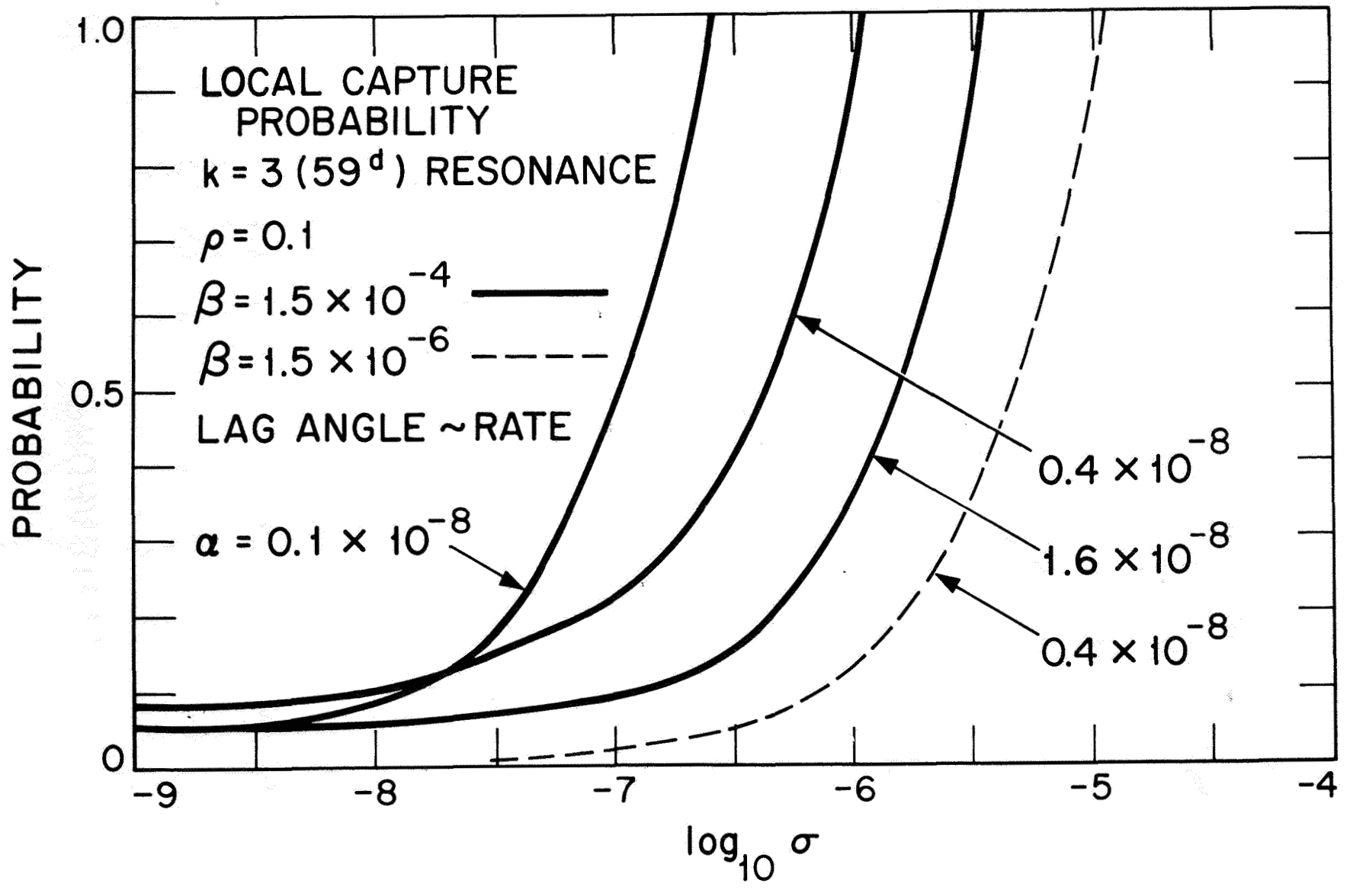


Thesis Figure 6

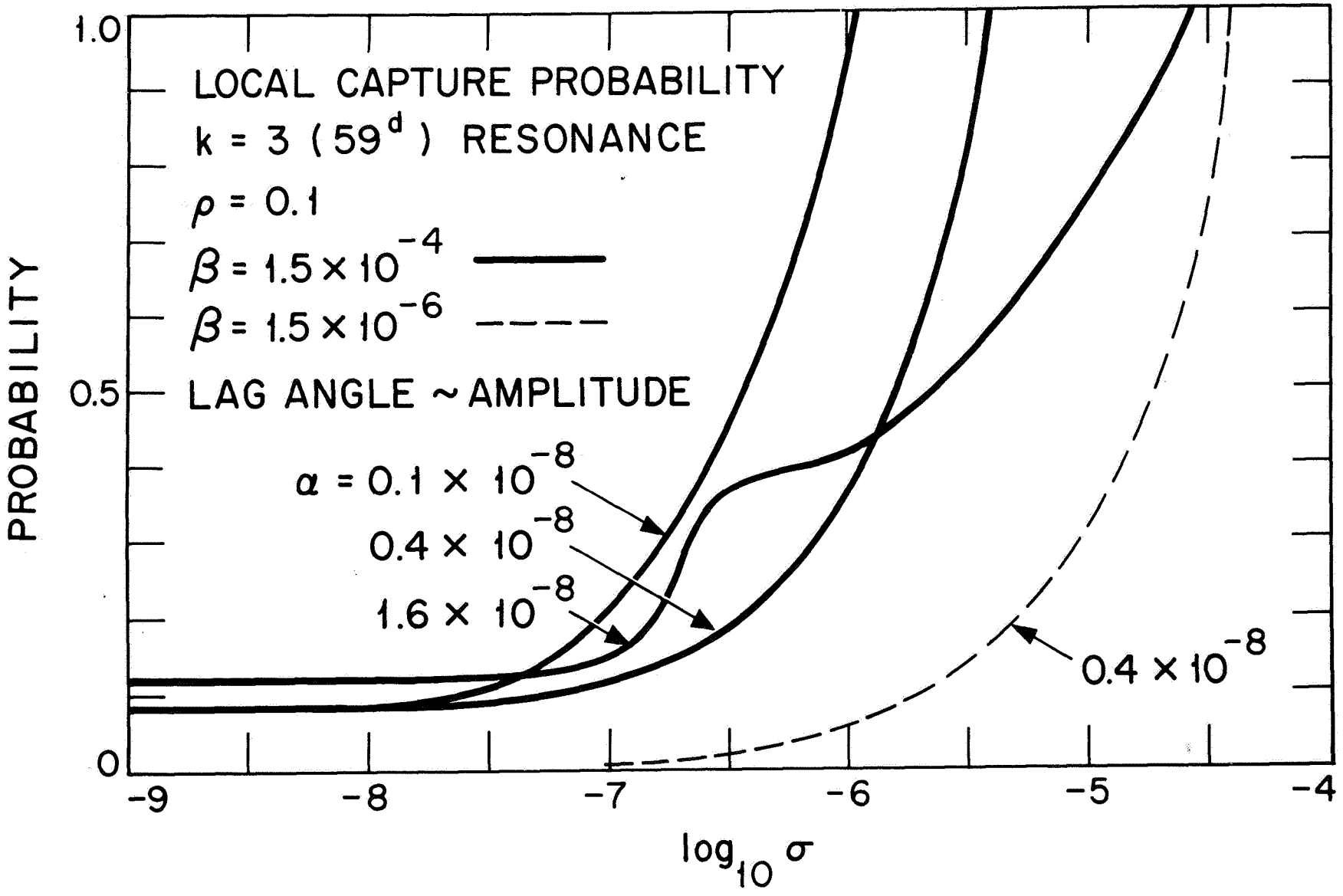


Thesis Figure 7

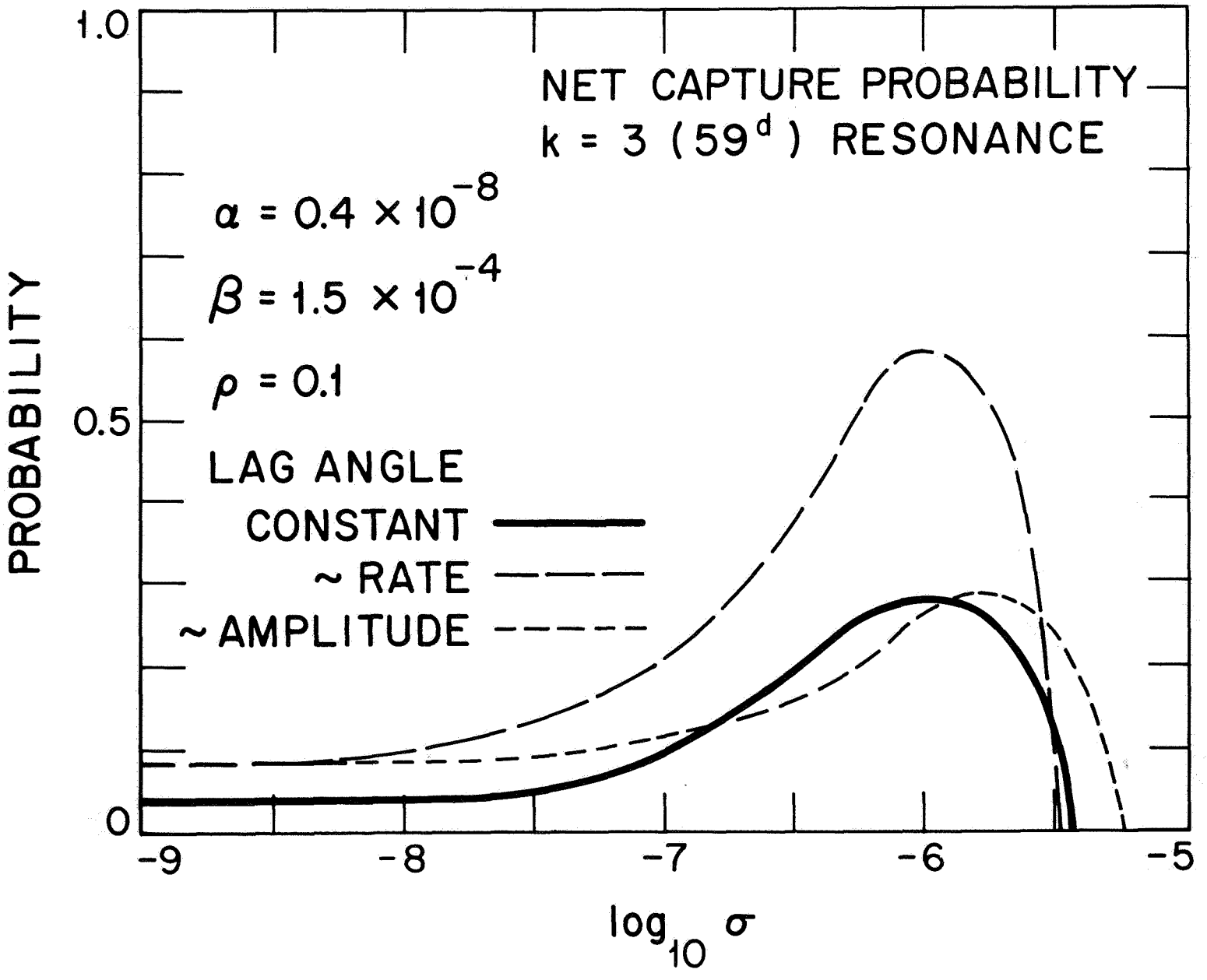


Thesis Figure 8

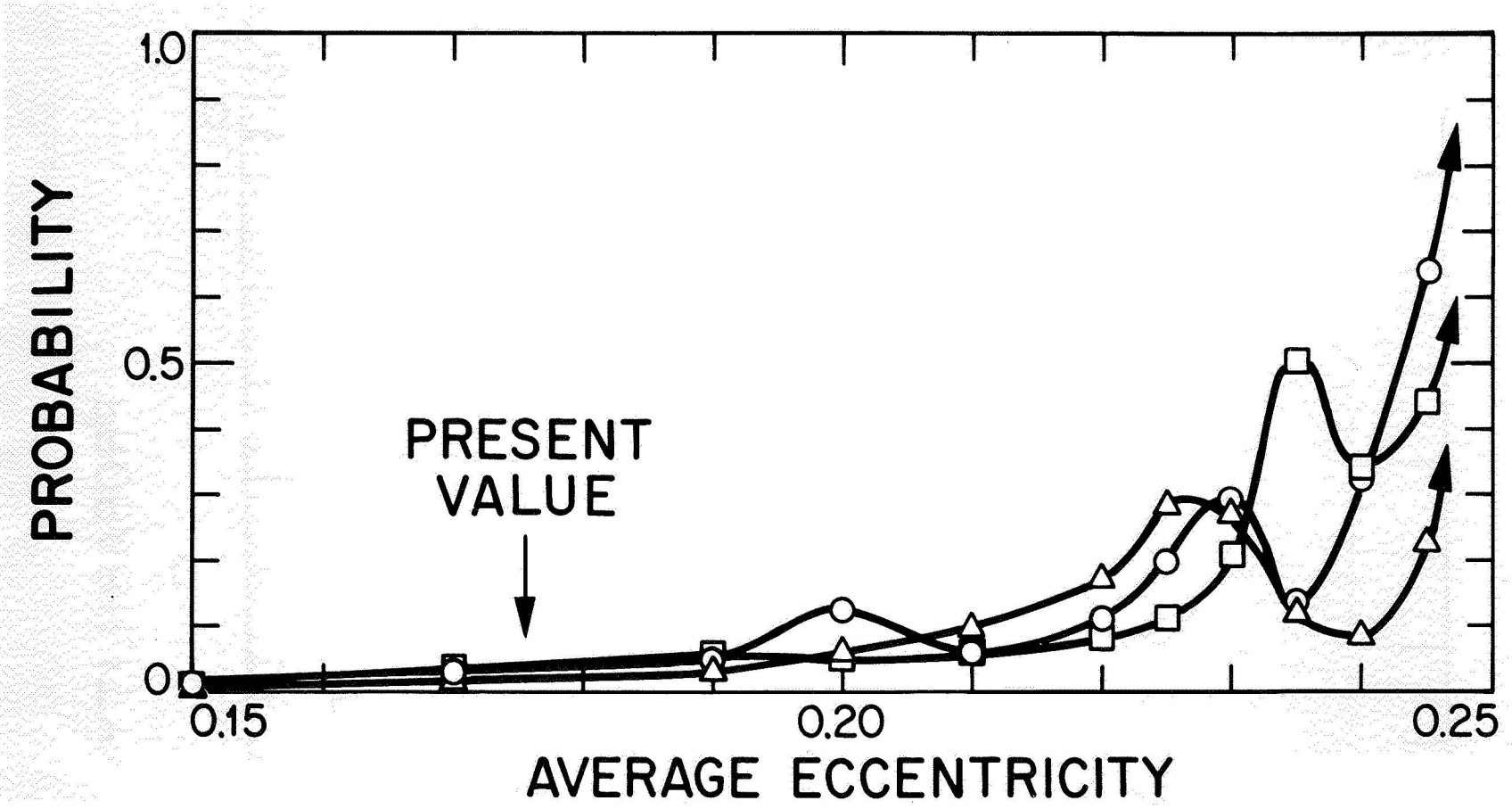


Thesis Figure 9